NICHOLE RENEE FOSTER
Laser Induced Photodissociation Studies of Novel Organometallic Complexes
(Under the direction of MICHEAL A. DUNCAN)

Gas phase complexes of chromium - coronene, niobium - coronene, niobium - pyrene, gadolinium - cyclooctatetraene and samarium - cyclooctatetraene are produced in a molecular beam using laser vaporization in a pulsed nozzle cluster source. Cation and neutral complexes are studied with time-of-flight mass spectrometry and mass-selected photodissociation. Clusters produced ranged from simple metal-organic adducts to metal-hydrocarbon and metal-carbide fragments. Mass spectrometry of Cr-coronene reveals formation of multi-decker sandwiches and a preference for binding to one side of the coronene molecule. Significant deviation from previously studied systems is observed for niobium - coronene and niobium – pyrene. Niobium is considerably more reactive with PAH species than other transition metals studied to date. Known solution phase sandwiches of Ln-cyclooctatetraene are also found to be produced as stable neutrals in the gas phase.

Index Words: PAHs, Coronene, Pyrene, Cyclooctatetraene, Transition metals, Lanthanide, Cation-pi interactions, Gas-phase, Organometallic chemistry, Interstellar-medium, Benzene complexes, Binding-energies, Sandwich structures, Photodissociation

LASER INDUCED PHOTODISSOCIATION STUDIES OF NOVEL ORGANOMETALLIC COMPLEXES

by

NICHOLE RENEE FOSTER

B.A., Augustana College, 1997

A Thesis Submitted to the Graduate Faculty of The University of Georgia in Partial Fulfillment of the Requirements for the Degree

MASTER OF SCIENCE

ATHENS, GEORGIA

2001

LASER INDUCED PHOTODISSOCIATION STUDIES OF NOVEL ORGANOMETALLIC COMPLEXES

by

NICHOLE RENEE FOSTER

Approved:

Major Professor: Michael A. Duncan

Committee: John Stickney
I. Jon Amster

Electronic Version Approved:

Gordhan L. Patel
Dean of the Graduate School
The University of Georgia
August 2001

DEDICATION

This is dedicated to my Grandma, Rosalie McLain, who died just as I was beginning my college career. Thank you, Grandma, for teaching me, among so many other things, that even in the most unfavorable conditions anything can sprout, bloom and bear fruit if it is well tended and looked after.

ACKNOWLEDGMENTS

There are so many!! I must first thank my advisor, Dr. Michael A. Duncan. You are absolutely magical in your ability to get people excited in the chemistry that we do. Thanks for pushing, prodding, cajoling and getting me through this! I'd also like to acknowledge my current and former lab mates Areatha Knight Ketch, Joe Velasquez, John Reddic, John Buchanan, Greg Grieves, Matt Nee, Angela Carroll, Todd Yaeger and Richard Walters. There is something so comforting in knowing that you are not the first or the last person who will have his or her head in the belly of a greasy, smelly diffusion pump and at the same time be covered in every organic solvent known to human kind! You all provided the much needed humor and conversation to make the work day enjoyable and sometimes even productive! Greg, you were so essential to this coming to fruition. Thank you for everything.

Thank you to my family and friends who have supported me throughout all of this. My mother, Charlotte Foster, who worried for me so that I didn't have to and for continually reminding me that I could do whatever I wanted and that really meant what I wanted. My father, Ed Foster, for your help with all of the cars I've had over the years. I will never forget screaming in your ear when I started Blueberry with a screwdriver while laying underneath it with the phone in my hand! You have both always communicated an enormous amount of confidence in me that made being strong a whole lot easier. Julia

Swancy, you are a Goddess! Thank you for laughing, crying, cussing, dancing, drinking,cloving and shopping with me! You are and will continue to be a very powerful force and dear friend in my life. Pat and Emily Ries, you are so fabulous! Thank you for all of those midnight runs to the beach, the endless cups of strong coffee and strong conversation. Thank you for being part of our chosen family and for being there for both of us through it all. To Tracy Cash and Cynthia Sanderson thanks for tons of giggles and relief from reality, not to mention many sweaty days on the softball field! Thanks to all of my neighbors on Bristlecone Ct., Karen, Karina, Marie, Heather, Alecia, Juanita, Dona, Tony, Robin, Nolan and Brittany. You were all so gracious and wonderful to me and Jess. We were like family! I will miss our block parties!

Finally, I must thank and acknowledge the two people who have made the end of this a possibility, Jessica McKee and Kai Exner. Jess, my sweet child, you are the light of my life. Having you gave me strength when I didn't have it, love when I needed it most, and the courage to keep trying when things didn't go as planned. Thank you for choosing me as your mother. I will always be grateful. And last, but certainly not least, Kai, my mate, you have become such a stabilizing force in my life! I have learned an enormous amount about life, love, patience, and of course, chemistry from you. We both know that I would not be here without you. Thank you for loving me the way that I deserve to be loved and for the family that you have helped me to create.

TABLE OF CONTENTS

Page

CHAPTER 1

INTRODUCTION

Almost every element in the periodic chart can form complexes with carbon and, yet, a compound of metal complexed with carbon was not identified until the mid to late 18^{th} century. It was then that Cadet de Gassicourt prepared and isolated methylarsenical, $(CH_3)_4As_2$. Around this same time Zeise Salt, $K^+ C_2H_4PtCl_3^-$ was isolated and reported by the Danish pharmacist after whom it was named. However, the actual structure of this compound remained unknown until the 1950s. The period of time between had one major discovery. In 1849, Edward Frankland prepared and isolated diethylzinc, $(C_2H_5)_2Zn$ which became the first organometallic reagent and dawned a new era in the expansion of organometallic chemistry. Diethylzinc and dimethylzinc remained the most utilized organometallic reagent until the beginning of the next century when Victor Grignard reported the synthetic uses of solutions of alkylmagnesium halides in ethers. His Grignard reagents quickly displaced diethyl- and dimethylzinc as the organic reagent. It was because of this discovery that molecules previously considered impossible to synthesize became easily produced. Shortly after that, organometallics were found to have uses outside the laboratory and became widely used in industry as gasoline additives, silicones, reaction catalysts, intermediates in polymer synthesis, medicinal compounds that lead to the advent of chemotherapy, and chemical warfare.[1,2]

The discovery of ferrocene in the early 1950s[3] and, shortly after, dibenzene chromium[4], were the next great discoveries in organometallic chemistry. This spurred an enormous increase in research into the area of novel organometallic chemistry with a change in focus from the uses in organic synthesis to the characterization of newly created complexes, emphasizing structure and bonding. The advent of gas phase spectroscopic techniques, such as laser vaporization techniques, ion beam mass spectrometry, collision induced dissociation, laser induced photodissociation, time

resolved IR spectroscopy, flowing afterglow, and photoelectron spectroscopy, developed in the 1980s opened this field to previously unrealistic synthesis possibilities. One heavily studied system in solution phase chemistry was metal-benzene. These systems were easily synthesized in the gas phase and found to create a plethora of novel complexes with interesting structural configurations. Freiser and coworkers used FT-ICR mass spectrometry to study these complexes with V, Ta, and Nb.[5] These studies provided bond energies and structural information, but were limited to complexes with one or two metal atoms and one or two benzene molecules. Bauschlicher and coworkers conducted theoretical studies on single atoms of the first and second row transition metals complexed with benzene and determined binding energies, structures and dissociation energies[6]. Our laboratory has studied the silver-benzene system and found charge transfer character upon photodissociation of the Ag-benzene cation.[7] In addition to charge transfer, our lab has also reported multiple metal – multiple benzene systems for systems containing V, Co, Fe, and Cu.[8] The silver system, in addition to complexes with transitions metals from titanium to copper, was studied with collision induced dissociation (CID) by Armentrout and coworkers.[9] More recently, Kaya and coworkers have used two-laser vaporization mass spectrometry and photoelectron spectroscopy to study M–benzene systems, where M = Sc, Ti, V, Cr, Mn, Fe, Co, and Ni. They have reported magic numbers that correspond to sandwich structures for complexes with the early transition metals vanadium, titanium, and scandium, whereas the late transition metals, i.e. iron, cobalt and nickel, adopt a benzene coated cluster type structure.[10] Ion mobility measurements by Bowers and coworkers have provided supporting evidence for the sandwich structure in the $V_n(C_6H_6)_{n+1}^+$ complexes.[11]

The discovery of C_{60} in the early 1990s by Smalley and coworkers provided yet another new and exciting organic ligand to introduce into gas phase studies.[12] Kaya has studied M-C_{60}, where M = Sc, Ti, V, Cr, Fe, Co and Ni, and again found magic numbers for these systems. They have proposed a stacked, dumbell configuration for the magic number corresponding to $M(C_{60})_2^+$ complexes where M = Sc, Ti, and V, and proposed a tricapped planar structure for the prominent $M(C_{60})_3^+$complexes observed when M = Cr, Fe, Co and Ni.[10] Martin and coworkers have reported that complexes of M_x-(C_{60}), for M = Ti, Zr, V and Y and x up to as many as 200 atoms, have metal coated fullerene structures.[13] Their studies of niobium and tantalum with C_{60} show metal atom insertion and efficient destruction of the fullerene cage.[14] The ion mobility studies of Jarrold and coworkers on Nb-C_{59}^+ show that the niobium atom is inserted into the fullerene network.[15] Our lab has published mass-selected photodissociation studies conducted on M_x-C_{60}^+ for M = Co, Fe, Ni, Nb, Ag, V [16] and competitive binding studies using mixed ligand sandwich complexes of iron with benzene, coronene and C_{60}.[17,18] These competitive binding studies showed that the relative binding strength of organic ligand to iron is coronene > benzene > C_{60}.

A relatively new area of novel organometallics involves metals bound to polycyclic aromatic hydrocarbons (PAHs). Dunbar and coworkers were the first to combine metals and PAHs in the gas phase.[19] They studied the association kinetics of various atomic metal ions with coronene and tribenzocyclene (an isomeric structure of coronene, $C_{24}H_{12}$) complexes using FT-ICR mass spectrometry. However, these studies were limited to single metal atom complexed with one or two PAH molecules. Subsequently, our lab has investigated a number of these systems using laser vaporization of a PAH-coated metal rod coupled with mass-selected photodissociation spectroscopy.[20]

These systems were found to produce multiple metal - multiple PAH clusters when metal = Ca, Ti, V, Cr, Mn, Fe, Ni, Ag, or Bi and PAH = coronene or pyrene. Two chapters of this work are focused on the results of a portion of that investigation. Chapter 3 of this work discusses the results of the chromium-coronene study and chapter 4 will discuss the niobium-coronene and niobium-pyrene results.

Metals complexed with PAHs have become an interesting area of inorganic gas phase research for several reasons. One such reason is that theorists often employ PAH molecules as models representing a finite section of a graphite sheet. This facilitates the study of surface physisorption energetics and dynamics. Likewise, these systems may be used to model metal intercalated graphite or metal attachment to the walls of carbon nanotubes. A second reason for the increase in research of metal-PAH systems is their astrophysical significance.[21] PAHs have been proposed to be the carriers of the main unidentified interstellar bands (UIBs) or diffuse interstellar bands (DIBs) which have been observed in all parts of the galaxy. They are projected to account for 5-15% of the cosmic carbon and, therefore, are an abundant component of the interstellar medium (ISM). Recent studies, however, have shown that isolated PAH molecule spectra do not exactly match the astrophysical spectra.[22] Therefore, the focus has shifted to various PAH complexes, including metal-PAH systems, to explain these UIBs and DIBs. With the assistance of molecular beam techniques these types of systems are now easy to synthesize and study in an environment which closely mimics that of interstellar space. A final reason that these novel systems are being heavily investigated is that due to the multiple sites available for π bonding, metal-PAH complexes may produce a variety of novel organometallics with new structural patterns.

Gas phase production and study of novel organometallics is not limited to PAH ligands. The discovery of a condensed-phase uranium – cyclooctatetraene (COT) analog to ferrocene, dubbed uracene, in the late 1960s caused a research boom in the area of actinide organometallics.[23] The inevitable extension to lanthanide metal – COT condensed phase systems, where metal = samarium, neodymium and cerium, found that these complexes were sandwiches in solution with stabilizing solvent molecules.[24] Those solvent effects quickly dampened the enthusiasm of those working to create a stable, isolated "lanthocene" crystal. However, these systems are easily created in the gas phase where solvent effects are not an issue. Kaya and coworkers were the first to study these systems in the gas phase.[10] They reported sandwich stoichiometries for Ce, Nd, Ho, Eu and Yb. This is plausible since triple-decker sandwiches were determined as the structures of the solution phase Ce-COT and Nd-COT complexes.[25] They also found that the lanthanide metals with preferred oxidation states of +3 have similar photoelectron spectra with binding energies between 2.5 and 3.5 eV, and subsequently the metals with preferred +2 oxidation states have similar photoelectron spectra with slightly lower binding energies between 2.0 and 2.5 eV. Chapter 5 of this work will discuss the results of our lanthanide-cyclooctatetraene study. This study shows that the photodissociation spectra of a +2 oxidation state metal, gadolinium, and a +3 oxidation state metal, samarium, differ and is consistent with the idea of a stronger binding energy in the +3 systems.

As stated throughout the above introduction this work reports the results of three novel organometallic investigations which encompass five complexes. The five complexes discussed include Cr – coronene, Nb – coronene, Nb – pyrene, Sm – COT and Gd – COT. All of these complexes were produced using laser vaporization of a metal rod

that has either been coated with a sublimed film of PAH or reacted with organic vapor carried in the backing gas. This experimental procedure will be described in detail in the next chapter.

CHAPTER 2

EXPERIMENTAL

The cationic and neutral species probed in this study were synthesized in a pulsed nozzle cluster source and investigated with time of flight mass spectrometry. Further information about these complexes was obtained with laser induced photodissociation.

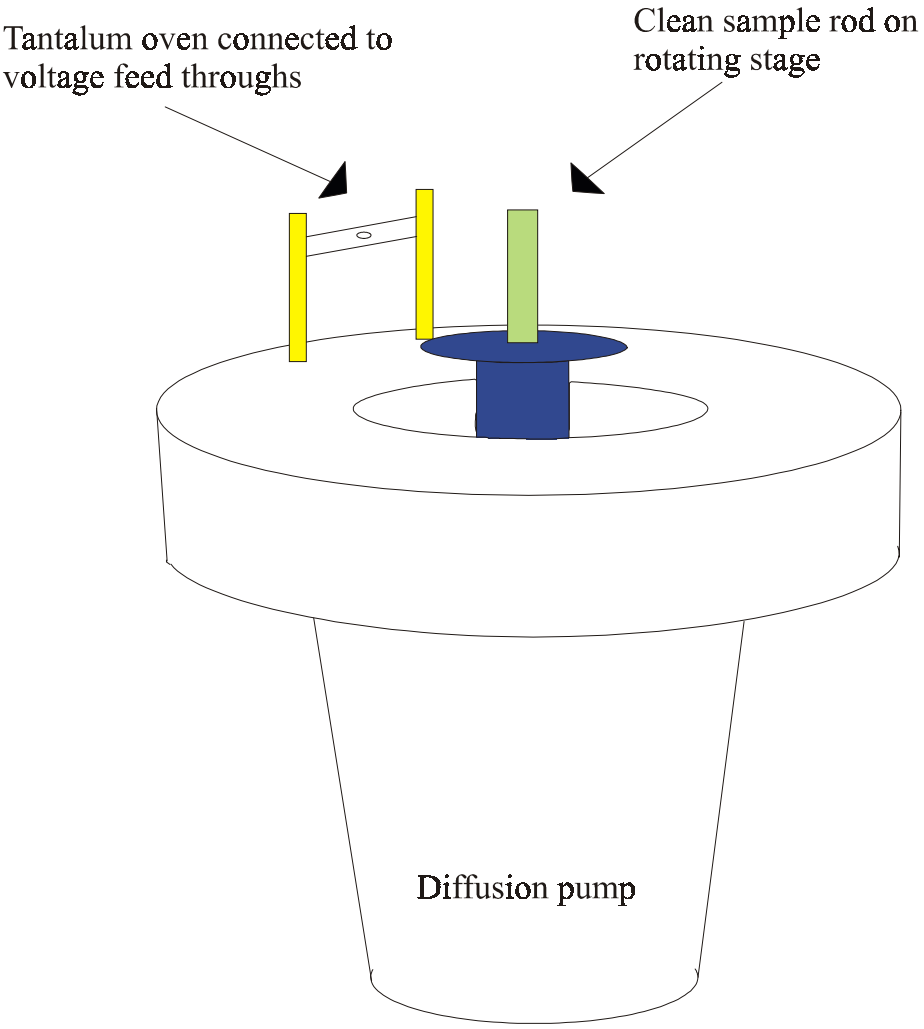

Figure 2-1: The rod coating apparatus

Coated rods are produced by vapor deposition in a vacuum deposition chamber (NRC model 3114) shown in Figure 2-1.[26] A very small amount of the PAH of interest is placed in a ¼ inch diameter tantalum oven. This oven is then attached to a variable resistance heater. The metal rod is placed upright on a rotating stage approximately 3-4 cm from the

orifice of the tantalum oven. The rotating stage is adjusted to allow the rod to turn at a rate of roughly 12-18 revolutions per minute in order to control the deposition uniformity. The chamber is sealed and evacuated to approximately $5x10^{-6}$ torr. The pumping system consists of a diffusion pump (Varian VHS-3) backed by a Welch Duo-Seal model 1376 mechanical pump. Once the system reaches the desired pressure the voltage applied to the tantalum oven is fixed at 40 V and the PAH is heated at a current setting of five amps. Deposition is normally complete after 10-20 minutes. The sample preparation chamber is vented and the rod is transferred to the cluster source assembly. When the organic being studied is not a solid at room temperature, clean rods are used and a volatile, liquid organic, such as cyclooctatetraene (COT) is seeded into the carrier gas. The COT is added to a holding cell in the He carrier gas manifold. The helium flows through the holding cell across the top of the COT and becomes seeded with COT molecules. Detection and study of the resulting complexes are carried out in the same manner as the coated metal rods.

The cluster source is housed in the first of two differentially pumped vacuum chambers of the molecular beam instrument[27], Figure 2-2. This initial chamber, dubbed the source chamber, is kept in the range of 10^{-6} to 10^{-7} torr by a diffusion pump (Varian VHS-10) backed by a Welch Duo-Seal 1475 mechanical pump. The cluster source is composed of a Newport pulsed molecular beam nozzle, rod holder, and nozzle extension(s), shown in Figure 2-3.[28] A metal rod, PAH-coated or clean, is threaded on to a stepper motor driven nylon screw which provides flexible translation and rotation of the rod within the holder. This allows laser ablation to occur on a continually fresh rod surface. The helium carrier gas flows through the pulsed nozzle and over the rod as the

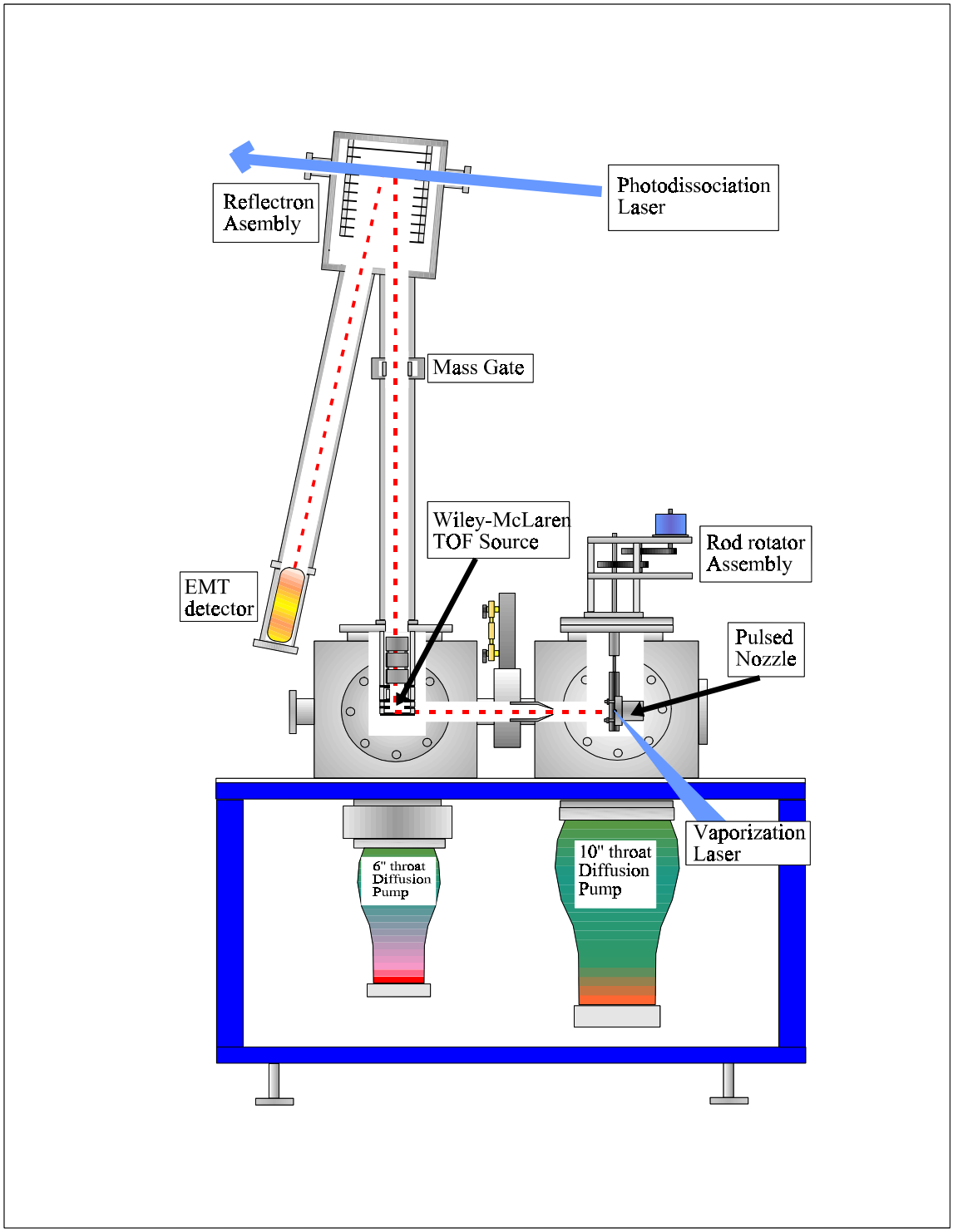

Figure 2-2: The molecular beam instrument.

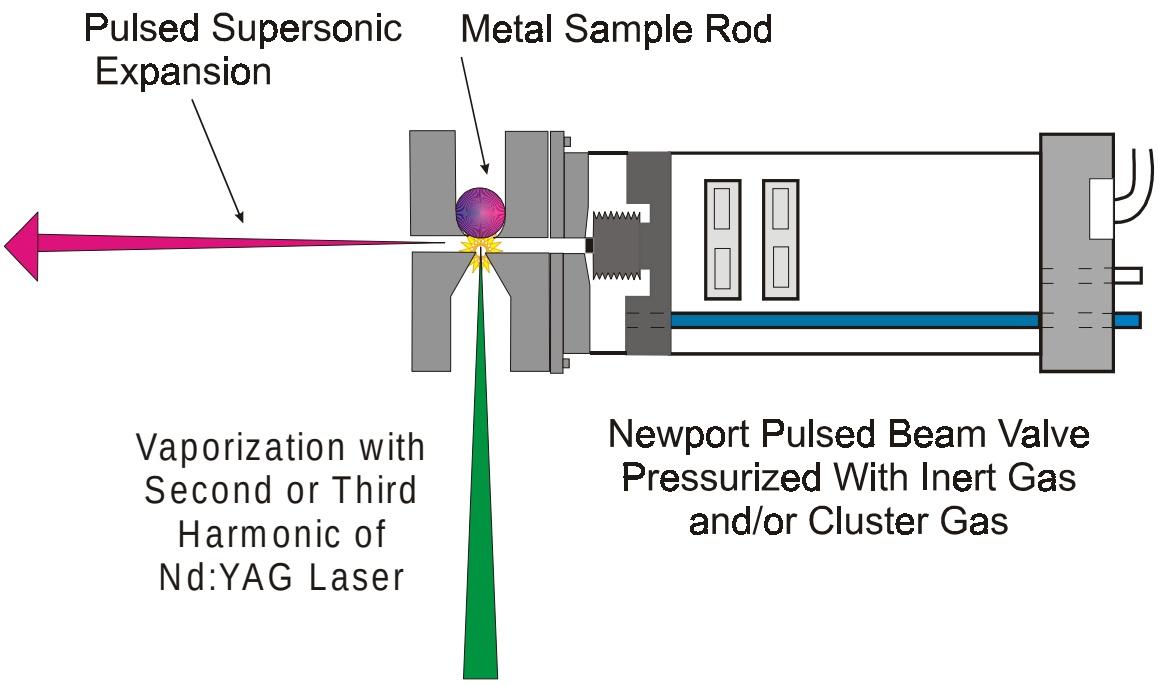

Figure 2-3: The pulsed nozzle cluster source.

ablation laser, a focused and power adjusted Nd:YAG laser operated at the second or third harmonic (532nm or 355nm), fires. The ensuing plasma is pulsed into the nozzle extension where multiple collisions occur and complexes grow. These complexes, along with the carrier gas, spray out the end of the nozzle extension into the vacuum causing cooling and providing a near collision free path into the second chamber, dubbed the mass spec chamber. Before entering this second chamber the center of the nozzle spray passes through a skimmer cone, thus creating a molecular beam with about a 3 mm diameter.

The mass spec chamber is kept in the range of 10^{-7} to 10^{-8} torr by a diffusion pump (Varian VHS-6) backed by a Welch Duo-Seal 1397 mechanical pump. This

chamber consists of the dual field, Wiley-McLaren type time of flight mass spectrometer coupled with a reflectron (RTOF)[29], and a Hamamatsu R-595 electron multiplier tube (EMT) detector.

Extraction of the species of interest from the skimmed molecular beam is accomplished by pulsing the acceleration plates in the mass spectrometer. The acceleration plates are operated in two distinct ways when experiments are conducted on neutral or ionized clusters. When neutral complexes are studied, the repeller is held at a potential of 1200 V and the draw-out-grid (DOG) is held at 1100 V. The DOG is a plate with a one inch diameter hole in the center that is covered with a molybdenum wire mesh. A third plate defines the beginning of the grounded flight tube. As the molecular beam enters the region between the center of the plates the ionization laser, a Lambda PhysikCompex ArF^+ excimer (193 nm), fires causing photoionization of the neutral species. These ions are immediately accelerated by the potential difference away from the repeller through the wire mesh of the DOG into the flight tube. These ions continue to accelerate due to the much greater field created between the DOG and ground plate. The second mode of operation is employed when ionic species are the subject of study. In this mode the repeller and DOG plates must be held at ground to allow ions to enter the extraction region. Once the cationic clusters have entered the region between the plates a pulsed potential accelerates them in the same manner as the photoionized clusters discussed above. The Wiley-McLaren construction provides not only extraction, but also causes separation of different complexes based on their velocities. The kinetic energy of a complex is equal to one-half the product of the mass multiplied by the velocity squared:

$$KE = 0.5mv^2$$

Solved for velocity, one obtains:

$$v = [2KE/m]^{0.5}$$

Therefore, the bigger the complex the slower the velocity it will have as it travels through the flight tube. This mass separation allows not only mass identification of the extracted clusters, but also allows further study of selected masses by laser induced photodissociation. After the deflection plates have corrected any directional deviation caused by the extraction process, the beam is squeezed tighter and made more uniform in diameter by the einzel lens. The beam then reaches the "mass gate". This is simply two parallel plates mounted in the flight tube approximately four feet from the mass spectrometer. It is held at a potential and simply deflects ions into the wall of the flight tube until the mass of interest arrives. A microsecond pulse to ground allows only that mass into the reflectron.

The reflectron is a stack of 14 plates one centimeter apart. A potential of 1380 V is placed on the stack during photodissociation. This creates an electric field that slows the ions, turns them toward the detector and re-accelerates them. It is at the turning point that a photoexcitation laser, a second focused Nd:YAG operated at the second or third harmonic (532nm or 355nm, respectively) is fired. The power of the laser is varied so that observations of nascent or sequential photofragmentation can be studied. The low power spectra are obtained at the threshold of fragmentation. Conversely, high power spectra show the most extensive fragmentation and are most certainly the result of multi-photon processes.

The photofragment and parent ion signals are collected at the end of a second flight tube by an EMT detector operated at 2.6-3.0 kV. The signal is amplified and sent

to a LeCroy digital oscilloscope (model 9310) where spectra are accumulated and then sent to a PC via IEEE-488 interface for analysis. The spectra shown in this work are presented in a computer difference mode in which the parent ion appears as a negative mass peak while its photofragments are plotted as positive peaks.

CHAPTER 3

CHROMIUM – CORONENE

Shown in Figure 3-1 is the mass spectrum of the chromium-coronene system. These cationic clusters are created by laser vaporization of a coronene coated chromium rod in the experimental manner discussed in the previous chapter. The peaks of highest intensity correspond to sequential adducts of metal atoms and coronene molecules. Weaker, unassigned peaks are metal oxides and coronene fragments. Metal oxides are unavoidable in this experimental setup. When rods are transferred from the coating apparatus to the source chamber they are exposed to the atmosphere and pick up surface impurities such as oxygen, water, sodium, etc. All of these minute impurities can be and are detected in the mass spectrometer. These complexes show series-like progressions which is a pattern observed in many of the metal-coronene systems we have studied.[20] The first such series is multiple metal atoms with one coronene. Within this series the most prominent peak is that of one metal with one coronene. Then follows a gradual decline in intensity with each addition metal atom. The last identifiable peak is that of Cr_5-coronene$^+$. This pattern holds for the second series of peaks, multiple metal atoms with two coronene molecules. Again, the prominent peak corresponds to that of the one chromium atom complex. A more rapid decline in intensity follows with a very weak peak at 860 amu corresponding to Cr_5-coronene$_2^+$. However, for complexes with three coronene molecules the pattern is different. There is a slight enhancement of the Cr_2-coronene$_3^+$ peak and the largest cluster detectable has only four metal atoms, not five. This enhancement holds over a variety of different mass spectrometer focusing conditions. This M_2-ligand$_3$ stoichiometry has been previously observed by Kaya and coworkers for a variety of metal-benzene clusters[30]. They have suggested that this stoichiometry has a double-decker sandwich configuration. Not shown in this spectrum

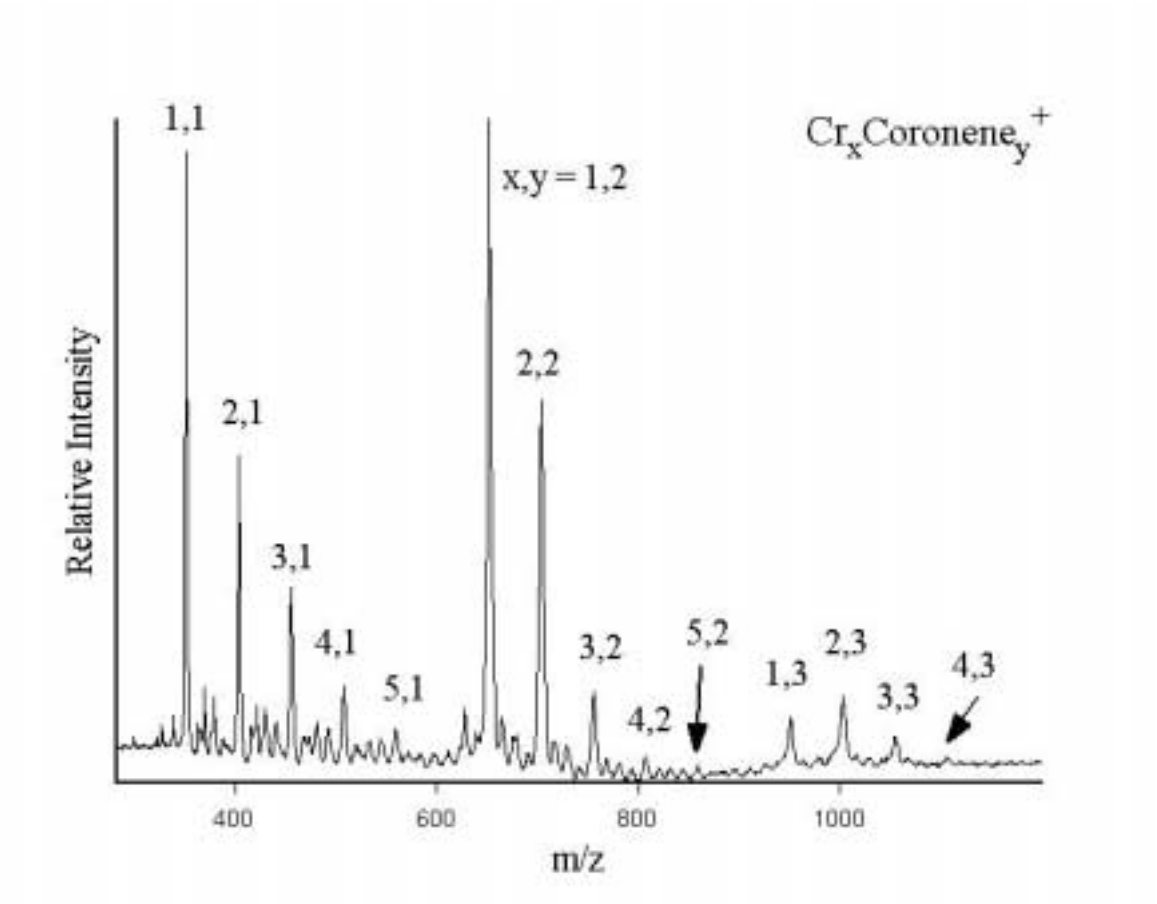

Figure 3-1: The Mass Spectrum of Chromium-coronene recorded at 532 nm.

is the lower mass region. There were no metal clusters in this region, only the rod surface impurities mentioned above. The source conditions were observed not to be conducive to metal cluster growth suggesting that the metal atoms in these complexes are added one by one, and not as clusters, to the coronene surface.

The structure of these complexes is an interesting question. Metal atoms could bind to the coronene at individual binding sites or, instead, they could form small clusters of metal on the surface, effectively binding metal to metal once one metal atom has attached to the coronene surface. The preferred binding scheme depends on the relative strengths of the two types of bonding, metal to metal or metal to organic. An equally

interesting and somewhat parallel question is whether bonding occurs on one side of the coronene molecule or both. Although the size of the chromium atom changes with its effective oxidation state, reasonable estimates suggest that three chromium atoms fit nicely to cover one side of a coronene molecule. Therefore, any cluster having more than three metal atoms would either have to have metal on both sides or have clustered metal on one side. With no convenient spectroscopic methods, we have employed mass-selected photodissociation experiments to probe these possibilities.

Species	IP (eV)	D_0 (cation)	D_0 (neutral)
Cr	6.7665	-	-
Cr_2	6.999	1.30	-
Cr_3	-	2.01	-
Cr_4	-	1.04	-
Cr_5	-	2.34	-

Table 3-2: Ionization potentials (IP) and dissociation energies (D_0) for relevant chromium clusters.

A table of known ionization potentials and bond energies for relevant chromium clusters is provided in table 3-2. The dissociation energy for many chromium clusters has been determined by collision induced dissociation.[31] However, the ionization potentials are known only for the atom and dimer.[32] Therefore, no method for deriving the neutral bonding energy for these clusters is available. It is usually true that the

ionization energy decreases with size for metal clusters and it is then plausible to assume that all the chromium clusters in this study will have lower ionization energies lower than that of coronene (7.29 eV). Using that assumption all of the metal clusters eliminated as photofragments in the dissociation will be charged and appear in the resulting photodissociation mass spectrum.

Figures 3-2 through 3-8 show the photodissociation mass spectra of the clusters observed in Figure 3-1. These clusters were studied at both 355 nm and 532 nm. At each wavelength and for each cluster the photodissociation laser intensity is varied to observe any changes in the fragmentation pattern. These laser power dependence studies show significant variation in fragmentation indicating that these processes must be multiphoton. This is not unusual or unexpected. Large molecules, such as coronene, have an enormous ability to internally convert electronic excitation energy and to continually cool themselves to the ground electronic state. Likewise, the unimolecular rate of dissociation for such a molecule would be slow. It would likely take excitation energies well beyond the dissociation threshold to see fragmentation on the microsecond time scale of our instrument. Multiple photons are needed to accomplish this and for fragmentation to be observed. It is therefore impossible to control the energy put into these systems and to distinguish between fragmentation pathways that occur sequentially or parallel to one another. Also seen in the following spectra are some peaks that are broadened beyond the normal instrument resolution. These are thought to arise from metastable fragmentation in which the dissociation time is slow compared to the residence time in the acceleration field. Considering the slow rate of dissociation for coronene this is not unexpected.

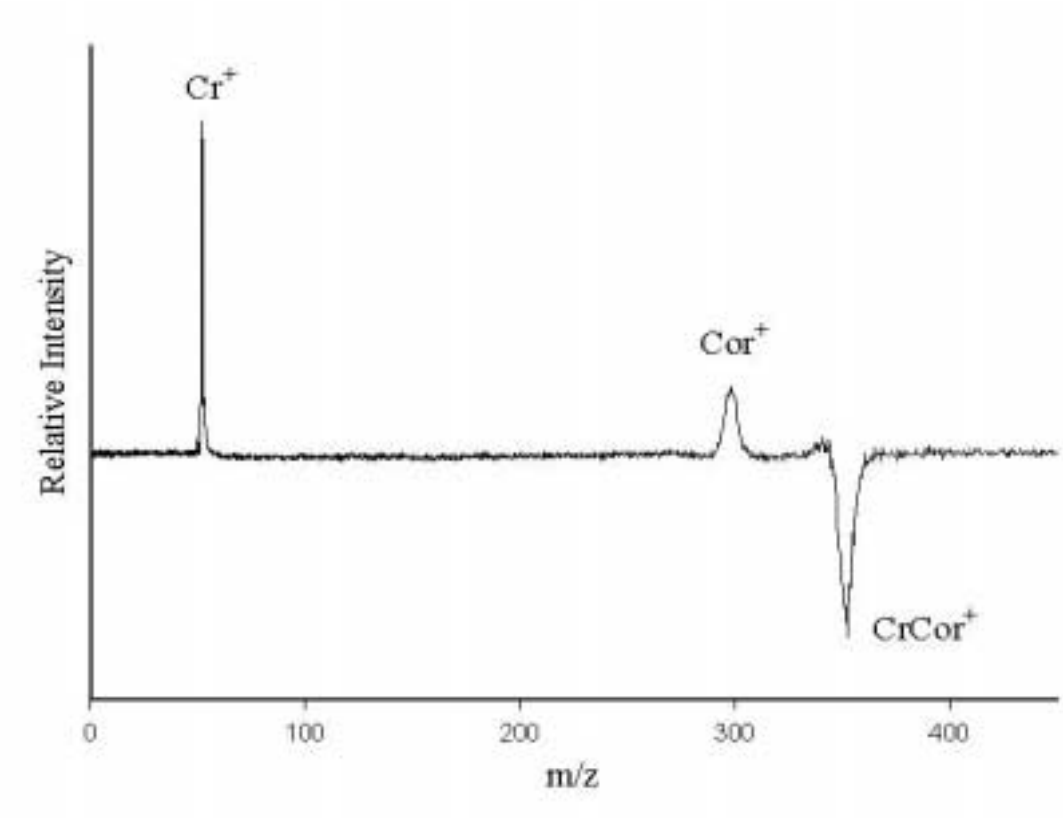

Figure 3-2: The photodissociation spectrum of Cr-coronene cation.

The photodissociation mass spectrum of Cr-coronene$^+$ is shown in Figure 3-2. Surprisingly, both the chromium atom and coronene molecule are observed as charge carrying photofragments. One would expect from the ionization potentials of chromium (6.77 eV) and coronene (7.29 eV) that the lower of the two, chromium, would be the only charged photofragment. The observation of coronene cation as a photofragment leads one to believe that the excitation energy was high enough to access a charge transfer asymptote. This is indeed a possibility when the high photodissociation laser energy input is considered (532 nm, 2.33 eV or 355 nm, 3.49 eV). However, this phenomenon of apparent charge transfer disappears at the low power limit of dissociation (not shown). At that point, the expected Cr^+ is the only observed photofragment. The presence of

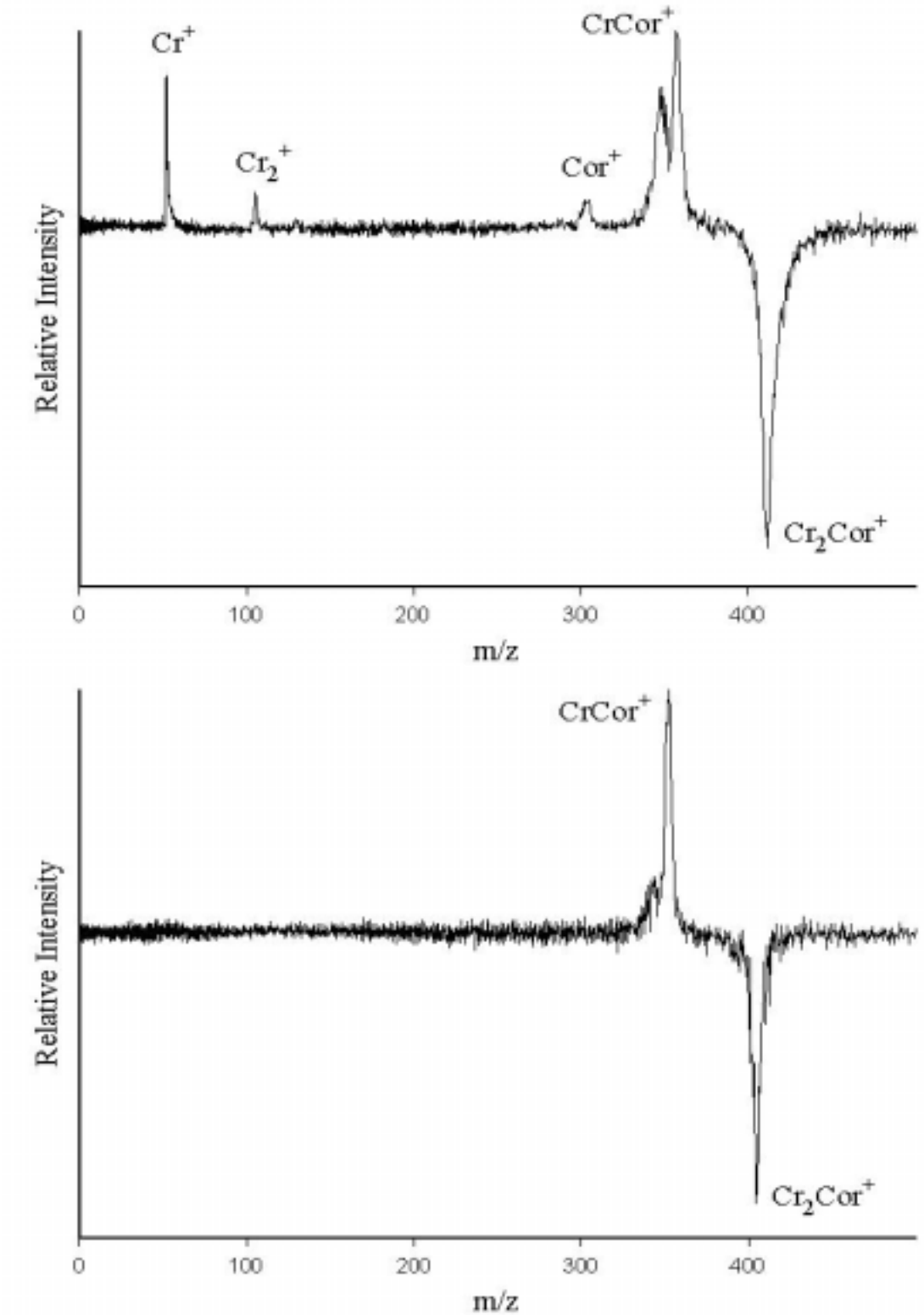

Figure 3-3: The photodissociation spectra of Cr_2-coronene$^+$ at low (upper trace) and high (lower trace) laser power

coronene cation observed here is more likely to be the result of neutral coronene photofragments being reionized by the multiphoton environment necessary for photodissociation. This is a common problem in systems like these where such high laser fluence is necessary for fragmentation. It is a recurrent feature in many of the following spectra.

Figure 3-3 shows photodissociation of Cr_2-coronene$^+$ at low (upper trace) and high (lower trace) power. The most prominent photofragment observed in the upper trace is Cr-coronene$^+$. This fragment results from the loss of Cr neutral from the parent ion and therefore suggests that Cr-coronene$^+$ has a lower IP than that of Cr^+ (6.7665 eV). A small, broad shoulder is observed at 340 amu. Although it is difficult to assign with certainty due to the broadening of the peak, it is thought to be the parent ion minus the fragment CrC. The shoulder peak is observed in any spectra in which Cr-coronene$^+$ is produced as a photofragment. The presence of this peak, which grows in intensity with higher laser power, indicates that at least some of the metal atoms have become strongly bound to the coronene molecule. In effect, they have become inserted into the ring system. Insertion of niobium atoms into coronene and pyrene[33] will be discussed in the next chapter and insertion of niobium[34] and iron[35] atoms into the walls of C_{60} has previously been reported. The high power trace shows more extensive fragmentation. In addition to the prominent Cr-coronene$^+$ fragment and a more prominent shoulder peak, there is also a strong Cr^+ peak. This peak could arise either from sequential fragmentation of Cr-coronene$^+$ or from reionization of the neutral chromium fragment produced in the initial photodissociation. Also present is a small coronene$^+$ peak as discussed previously and a small amount of Cr_2^+. The latter cannot be produced by sequential fragmentation of Cr-coronene$^+$ and, therefore, must represent a parallel

dissociation pathway. The presence of the dimer cation also suggests that there must be more than one isomer of the parent ion. In this isomer the metal is not inserted into the ring system, but more weakly interacting.

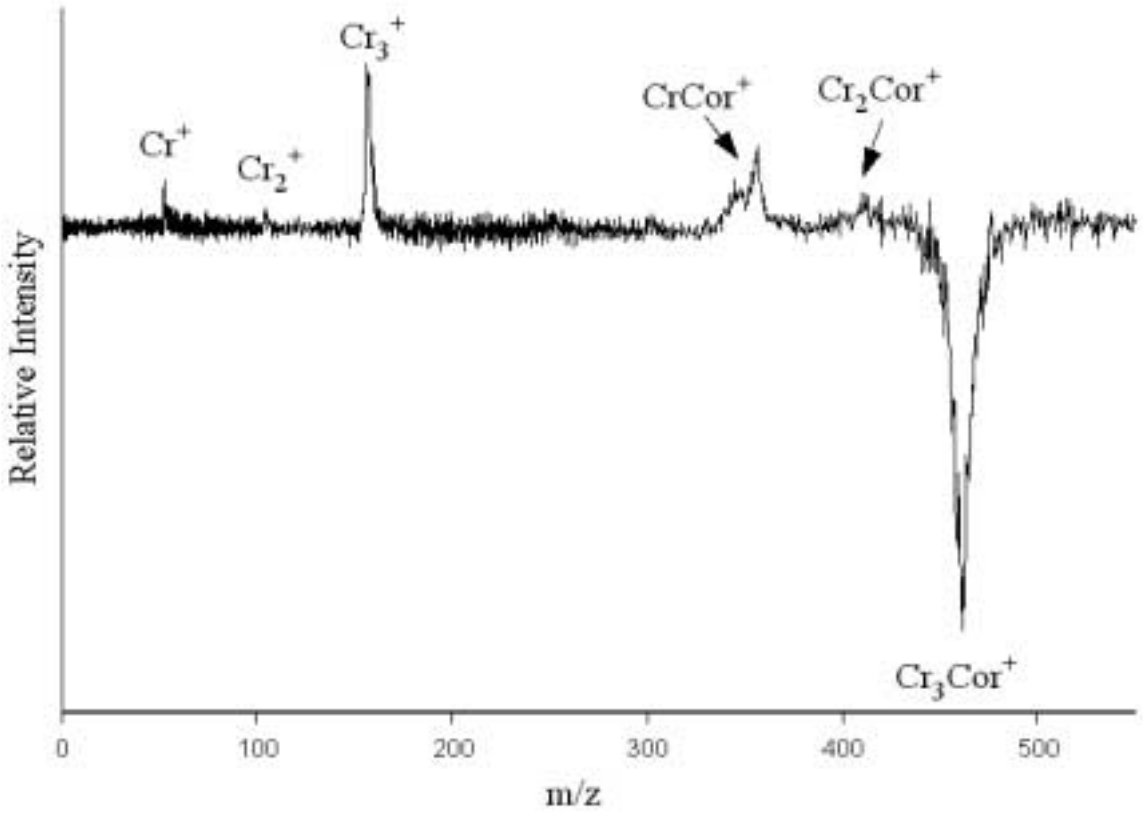

Figure 3-4: The photodissociation spectrum of Cr_3-coronene$^+$ at 355 nm.

Figure 3-4 shows the photodissociation of Cr_3-coronene$^+$ at 355 nm with moderate laser power. Again we see two distinct dissociation pathways, one which produces Cr-coronene$^+$ and its sequential photofragments along with the familiar shoulder peak and another which produces the chromium trimer cation. The appearance of dimer and atomic metal cations are observed to be laser power dependent. As laser power is lowered they weaken in intensity until, at the lower limit of dissociation, they disappear

suggesting that they are produced by further fragmentation of Cr_3^+. The low power limit spectrum (not shown) has one fragment ion peak, Cr_3^+. The presence of metal trimer elimination here and the dimer cation in the previous spectrum indicates that in at least some, if not all, of these Cr_x-coronene$^+$ complexes, all of the metal atoms are located on the same side of the coronene molecule. It is highly unlikely that metal atoms from opposite sides could cluster efficiently before being eliminated.

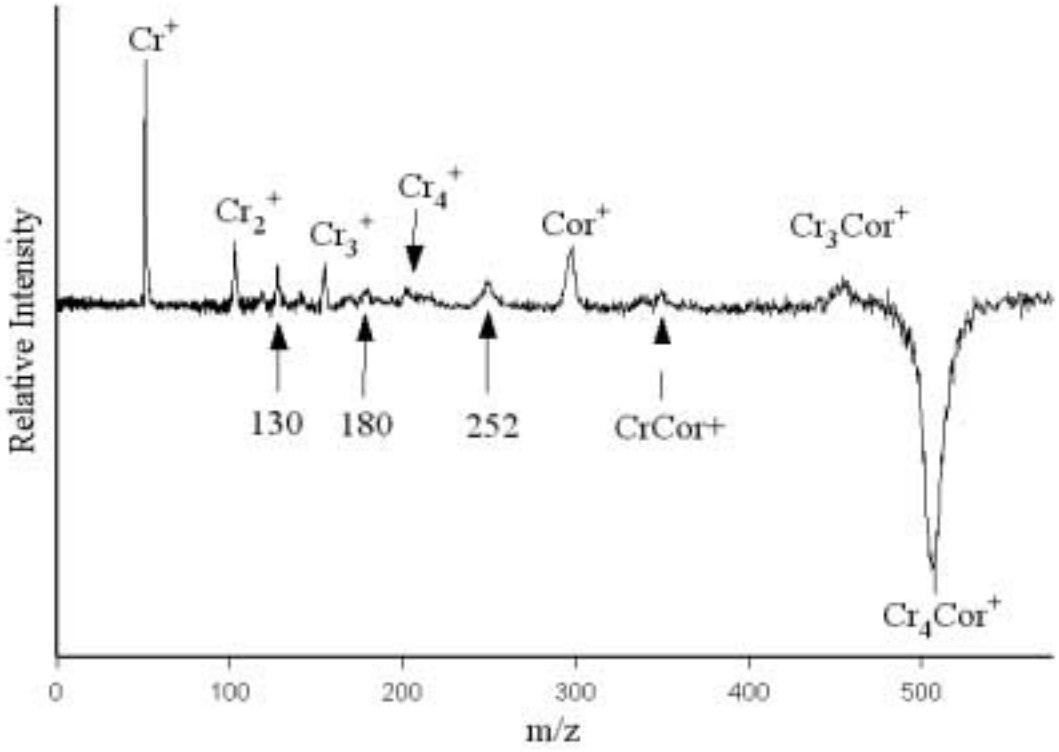

Figure 3-5: The photodissociation spectrum of Cr_4-coronene$^+$ at 355 nm.

The photodissociation mass spectrum of Cr_4Cor^+ is shown in Figure 3-5. This spectrum was obtained with 355 nm at high power. This complex is the largest multi-metal complex with enough signal to photodissociate. However, the signal is still weak and high laser power was necessary to see any fragmentation. The highest mass peak

seen is Cr_3-coronene$^+$ which is a broad, weak signal consistent with metastable fragmentation. The remaining peaks are similar to the fragmentation pattern of Cr_3-coronene$^+$. These are probably produced by sequential fragmentation of this metastable cation. Other coronene containing fragments are the coronene cation itself, more than likely reionized neutral coronene as discussed with Figure 3-2, and Cr-coronene$^+$, similar to that seen in the previous spectrum. However, there is a noted absence of Cr_2-coronene$^+$ as a fragment ion. This combined with the metastablility of Cr_3-coronene$^+$ complexes denotes some enhanced stability in the three metal atom complex. This is in agreement with the three chromium atom per side geometric motif. Another interesting facet of this spectrum is the appearance of a small Cr_4^+ peak. This peak supports the notion that the chromium atoms bind to the same side of the coronene. This fragment peak does, however, have a second possible identity as discussed below.

A number of new features appear in this spectrum that cannot be assigned as any multiple of metal and coronene . Peaks at 130, 180, and 252 amu have not been observed as fragment ions in any of the other multi-metal complexes. These peaks correspond to organometallic fragments from a dissociated coronene ring system. Mass 130 corresponds to Cr-benzene$^+$ and mass 180 to Cr-naphthalene$^+$. The broadened peak at 252 is approximately the same mass as Cr-pyrene$^+$ or it can also be formed by eliminating neutral dibenzene chromium (208 amu) from the parent ion. Also worth noting, the peak which is labeled as Cr_4^+ occurs at this same mass, 208 amu. This peak could then also be assigned as Cr-$(benzene)_2^+$. Unfortunately, these signals are weak and broad and the mass resolution is low. The uncertainty is approximately 1-2 mass units. The

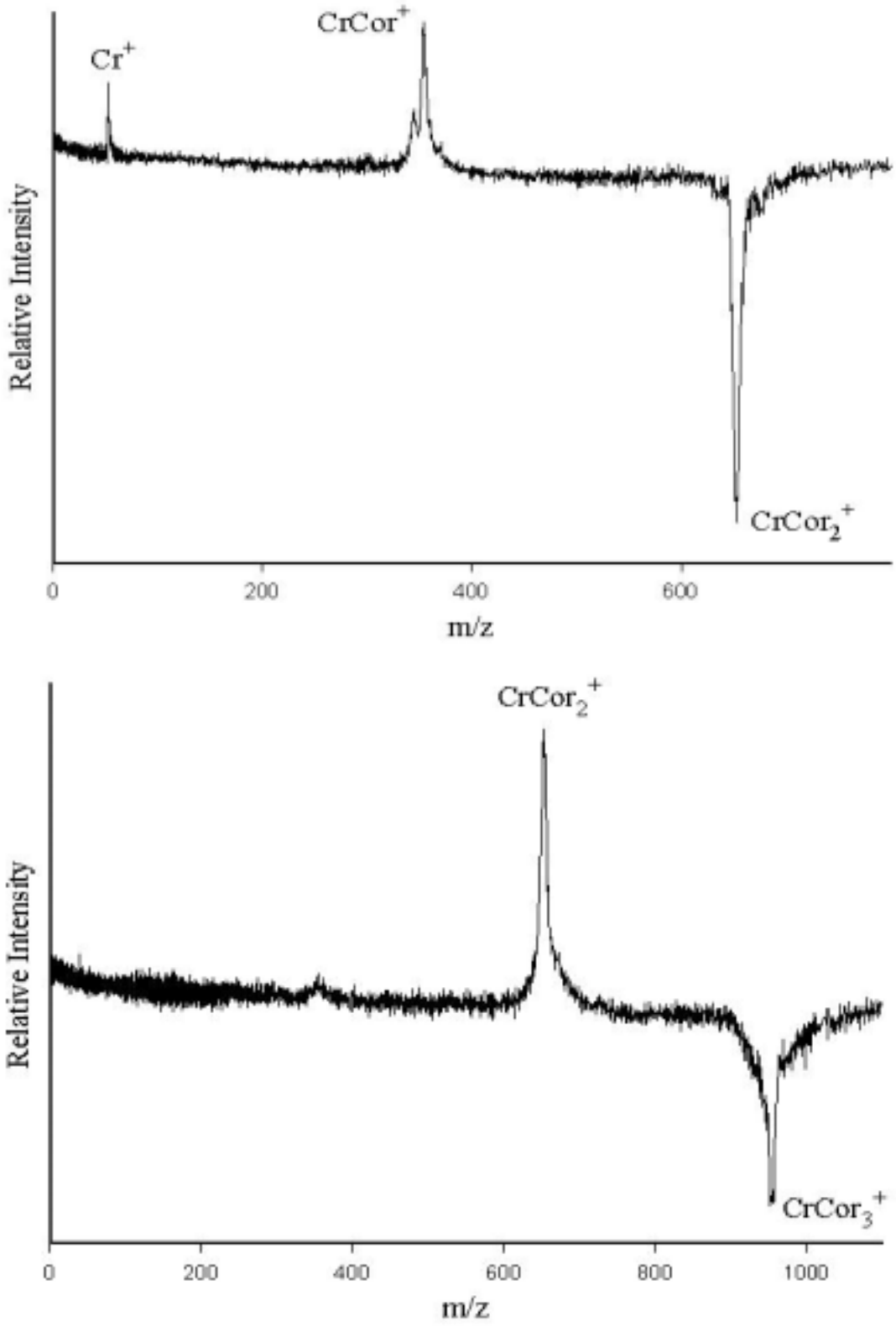

Figure 3-6: The photodissociation spectra for Cr-coronene$_2^+$ (upper trace) and Cr-coronene$_3^+$ (lower trace) at 532 nm.

fragmentation of metal-coronene into smaller organometallic fragments is not unlikely. Extensive rearrangements are likely due to the high energy requirements of such a process. What is truly interesting is that these fragments only appear when the cluster contains four chromium atoms even with the high laser powers used on complexes with fewer chromium atoms. The presence of at least four chromium atoms seems to be a necessary requirement to open these new fragmentation pathways. The idea of a necessary number of metal atoms for ring destruction has been reported previously in the photodissociation of metal-C_{60} complexes.[14]

Figure 3-6 is the photodissociation spectra obtained for Cr-coronene$_2^+$ (upper) and Cr-coronene$_3^+$ (lower) at 532 nm. The Cr-coronene$_2^+$ peak was a prominent peak in the original mass spectrum of ions created in the source. This apparent stability together with the stoichiometry suggests that it has a sandwich type structure. The sandwich structure is also supported by the absence of pure coronene cluster formation in the original distribution. It appears that the presence of chromium atoms is a necessary requirement for coronene to aggregate. Once this complex has formed high laser power is necessary to dissociate it. The only fragments of this complex observed are Cr-coronene with the 340 amu shoulder and chromium cation. In the lower trace, we see that the Cr-coronene$_3^+$ parent ion fragments almost exclusively into Cr-coronene$_2^+$ with a very small amount of Cr-coronene$^+$. The strong peak intensity of the Cr-coronene$_2^+$ fragment here provides more evidence that it is indeed a sandwich structure. In experiments not shown, the system was seeded with acetone to test for any exposed metal. In those experiments, this suspected sandwich complex, Cr-coronene$_2^+$, did not react with the acetone, but all Cr_x-coronene complexes did as they must certainly have

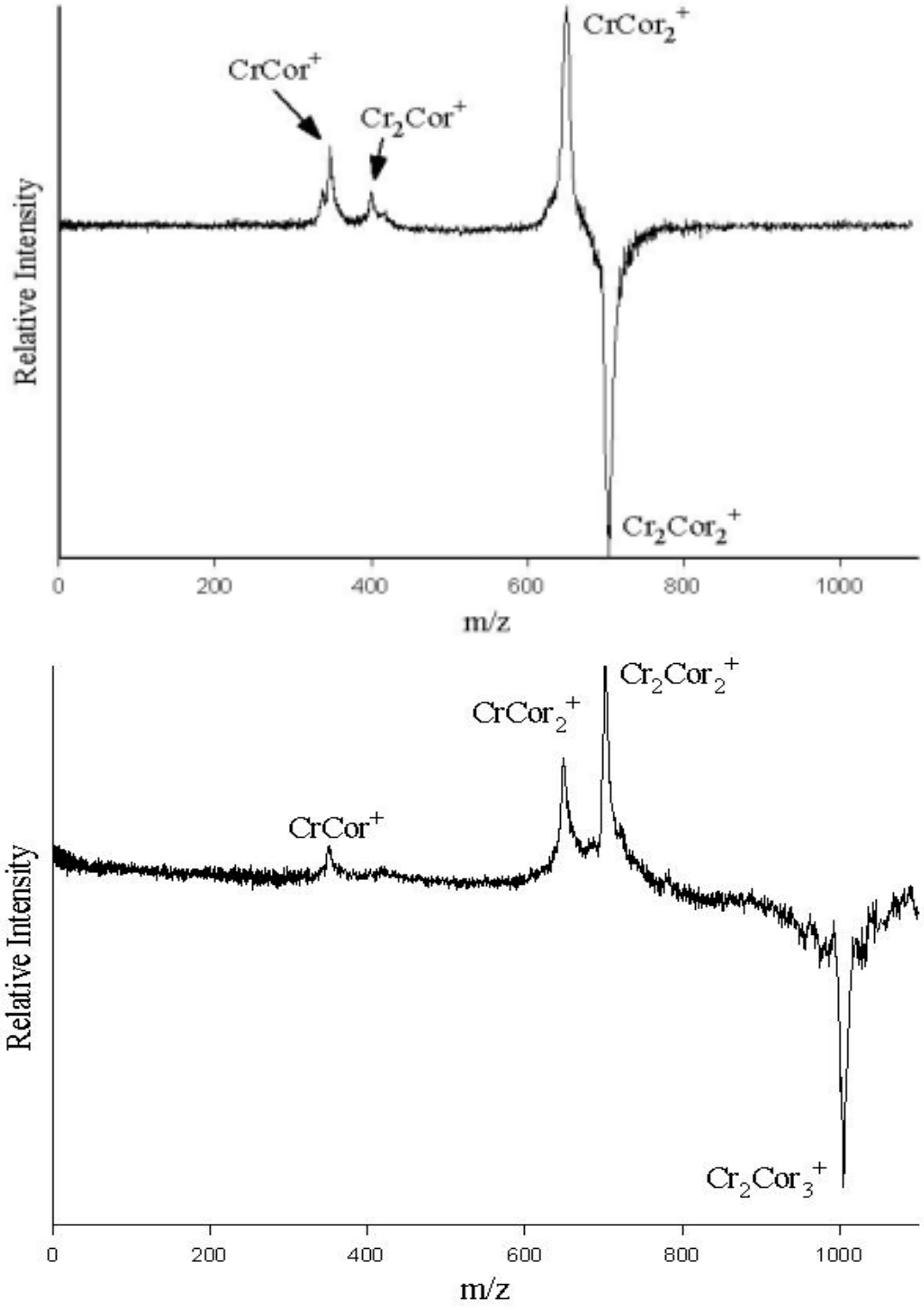

Figure 3-7: The photodissociation spectra of Cr_2-coronene$_2^+$ (upper trace) and Cr_2-coronene$_3^+$ (lower trace) at 532 nm.

exposed metal. This is consistent with the idea that sandwich structures have protected metals which are not available for further bonding.

Figure 3-7 shows the photodissociation of Cr_2-coronene$_2^+$ in the upper trace and Cr_2-coronene$_3^+$ in the lower. There are two structural possibilities for the Cr_2-coronene$_2^+$ complex, one in which the metal atoms are sandwiched between the two coronene molecules or an alternating metal-coronene-metal-coronene structure. The prominent fragment peak observed is Cr-coronene$_2^+$. This supports the alternating metal-coronene motif. Moreover, in the previously mentioned acetone studies, Cr_2-coronene$_2^+$ did form an adduct providing evidence for this structure. The weak signal indicating the presence of Cr_2-coronene$^+$ would be produced by elimination of a coronene from the sandwich. This fragment would have exposed metal on both sides of the coronene molecule. Such a complex would be fairly unstable and dissociate easily into Cr-coronene$^+$. The Cr-coronene$^+$ peak was the most prominent fragment in the photodissociation of both Cr_2-coronene$^+$ and Cr-coronene$_2^+$, Figures 3-3 and 3-6 respectively. Therefore, it could be produced as a sequential fragment from either of those two higher mass fragments.

The lower trace shows the same fragmentation peaks with the exception of Cr_2-coronene$^+$. A reasonable structure would be a double decker sandwich motif in which there are alternating coronene-metal units. This constitutes a coronene-capped Cr_2-coronene$_2^+$ so that there is no exposed metal in this complex. These stoichiometries have previously been suggested for V_x-benzene$_y$ complexes and other multi-metal organometallics.[36] The fragmentation pattern shown supports this as well. First, the complex loses one of the outer coronene end caps. It then loses the exposed chromium leaving the single atom sandwich. Lastly, another coronene is eliminated leaving the stable Cr-coronene complex.

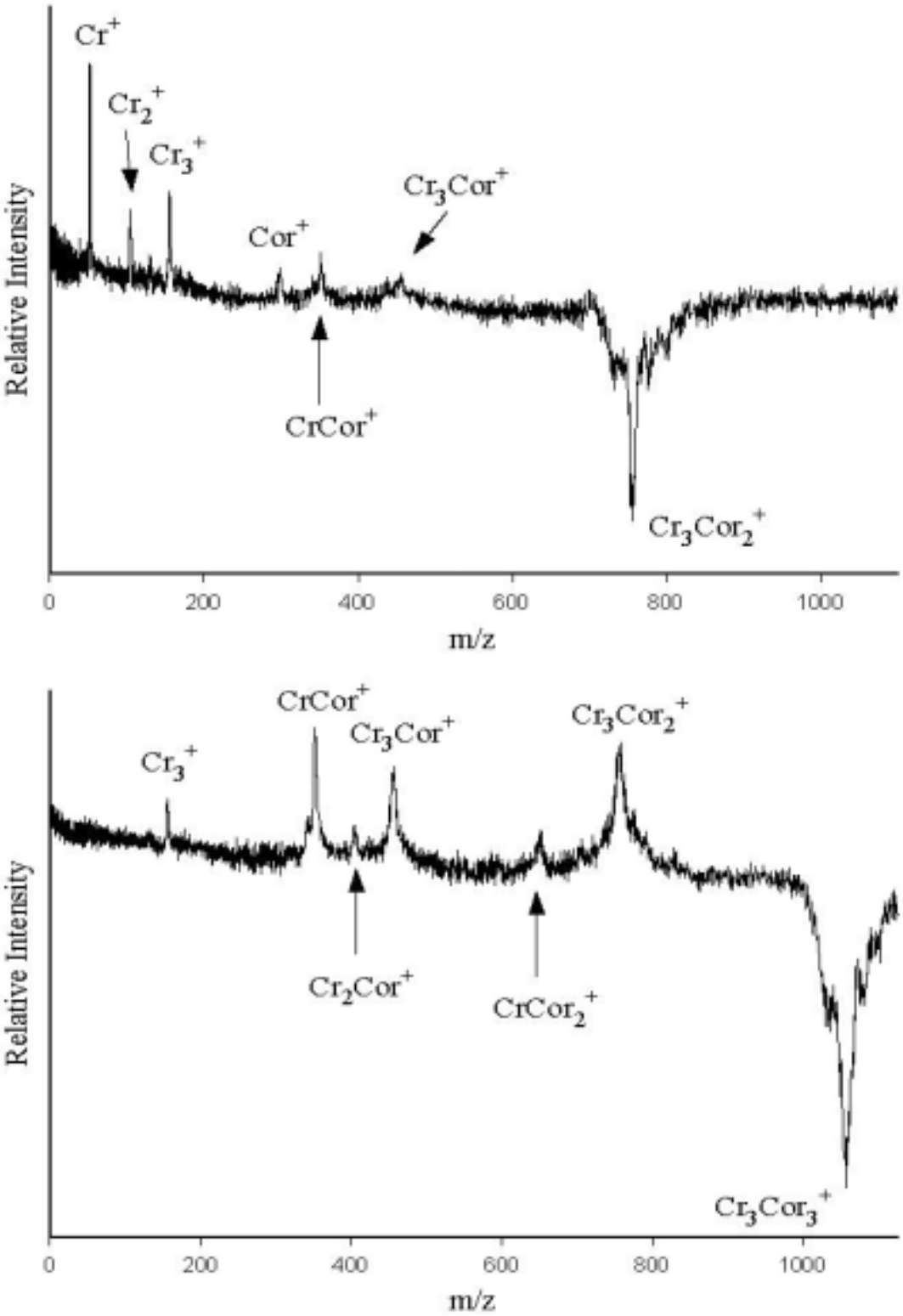

Figure 3-8: The photodissociation spectra of Cr_3-coronene$_2^+$ (upper trace) and Cr_3-coronene$_3^+$ (lower trace) at 355 nm.

The largest multiples observed for the chromium-coronene system are dissociated in Figure 3-8. The initial signal was weak and, therefore, high laser power was necessary to observe any fragmentation. There are a number of isomeric structures possible for such systems, but the dissociation spectra are fairly simple. The upper trace, Cr_3-coronene$_2^+$, has only one high mass fragment, a very weak signal at Cr_3-coronene$^+$. This fragment would be produced from the loss of coronene from the parent. This information together with the lack of any sandwich intermediates such as Cr_2-coronene$_2^+$ or Cr-coronene$_2^+$ is not consistent with the alternating sandwich structure motif. Instead, this is consistent with a sandwiched metal trimer. Further evidence for such an entity is the presence of Cr_3^+ as a fragment. A trimer sandwich was also the proposed structure for previously investigated Fe_3-coronene$_2^+$. The lower mass fragments are consistent with the fragmentation pattern observed in the Cr_3-coronene$^+$ photodissociation mass spectrum, Figure 3-4. Both complexes show reasonably high stability in that they are difficult to dissociate and fragmentation signal is very weak.

The lower trace provides more information about the stability and structure of Cr_3-coronene$_2^+$. If it is indeed a stable complex, then it should be a prominent mass fragment of Cr_3-coronene$_3^+$ and it is. In this spectra, as in the upper spectra, the fragments associated with the trimer sandwich breakdown are observed, as well as the stable Cr-coronene$^+$ and its shoulder peak at 340amu. There are, however, new features in this spectra. Here we see the above missing alternating sandwich intermediates, Cr_2-coronene$^+$ and Cr-coronene$_2^+$. These fragments are weak and could be present, but undetectable in the upper spectra. They represent an exact splitting of the parent ion into two parts. One part must be initially neutral, however, with the high laser powers used here reionization of that neutral photofragament is likely to occur. The interesting point

of these spectra is that for such large molecules with many possible isomers there are relatively few photofragments, and that the strength and stability of the trimer sandwich is evident in both. Also present in this spectra is evidence that there are indeed two isomeric structures of Cr_3-coronene$_3^+$ present in the molecular beam.

After many spectra it becomes difficult to discern what is important, but there is some fascinating information contained in this study. The most obvious is that chromium forms strong bonds to coronene. This is evident in the necessity for high laser power, multiphoton conditions to cause fragmentation and the observed chromium carbide elimination in some of the complexes. Coronene is known to bind strongly to metals. Previous work in our lab has focused on the competitive binding between metals and mixed ligands.[37] In that work, the mixed ligand complexes created, Fe-Coronene-R^+ where R = benzene or C_{60}, showed that during photodissociation benzene or C_{60} were eliminated first. Since the bond energy of Fe-benzene is known to be 49 kcal/mol, it can be deduced that the Fe-coronene bond is greater than this. The binding energy of Cr-benzene, 40 kcal/mol, is quite similar to that of Fe-benzene and it is therefore expected that the chromium-coronene bond also would be strong.

The evidence for preferential binding is another interesting fact obtained through this investigation. The prominence of metal cluster peaks throughout the work suggests that metal atom attachment occurs preferentially on one side of the coronene surface. It is possible that the metal clusters could form first and then bind to the coronene, but no evidence for metal clusters in the original distribution of ions out of the source exists. The source conditions and nozzle channel used for this study were not conducive to metal cluster production even when no coronene was present. Therefore, it seems that coronene is necessary for metal atoms to cluster and that these complexes grow from

sequential addition of metal atoms to the coronene surface. Although it has been mentioned that three chromium atoms fit nicely to cover one coronene side, it also makes sense that surface metal atoms would be available to bind with other metal atoms available in the source, just as surface metal atoms complexed with the acetone in the probe for unprotected metal atoms. The idea that three chromium atoms are ideal to cover one side is also consistent with NMR spectroscopy and theory which finds that the outer alternating rings of the coronene molecule have greater electron density.[38] These are more likely to bind to a metal atom than the center of the molecule. Binding to these outer rings has been observed in synthetic organometallic chemistry[39] and ab initio calculations agree that this type of binding is energetically favored[40].

This information has significant implications for the alternating sandwich structures. Although for Cr-coronene$_2^+$ a centered metal atom placed between two coronene is the first such construct that comes to mind, in reality this is not the most likely structure. The metal would bind, as discussed, to an outer ring of each coronene. The charge induction in both rings created by the newly bound metal would be of the same polarity causing the ends of the two coronenes to rotate away from each other creating a staggered conformation. The Cr_2-coronene$_3^+$ "double decker" sandwich would then have a "stair-step" motif. Illustrations of these possibilities, along with the trimer sandwich and Cr_3-coronene$^+$, are shown in Figure 3-9. Notice that the presence of a metal filling between the two coronenes necessitates a highly symmetric structure wherein there is no interaction between coronene molecules, only between metal and coronene. Although this data does not provide exact structural information the proposed structures are the simplest explanation for the observed fragmentation.

CHAPTER 4

NIOBIUM – CORONENE

AND

NIOBIUM – PYRENE

Shown in Figure 4-1 are the mass spectra for the niobium-PAH systems. The PAH is either coronene or pyrene. The cationic clusters in the upper trace are created by laser vaporization of a coronene coated niobium rod. Those in the lower trace are created using a pyrene coated niobium rod. All of the spectra discussed in this chapter are produced and photoexcited using the third harmonic, 355 nm, of a Nd:YAG. Both spectra show sequential adducts of metal atoms with PAH molecules. This has been seen previously with many of the metal-PAH systems we have studied.[20] However, these spectra are markedly different from the established pattern of these types of systems. There are a number of new features present in these spectra such as the presence of many metal-hydrocarbon and metal-carbide ions. These peaks can only be the result of fragmentation of the adducts being produced in the cluster source. Included in these ions is $Nb_4C_4^+$ which is known to be a magic number in niobium-carbide clusters.[41] Fragmentation of the PAH is conceivable considering the energetics of the laser plasma, but these conditions have rarely produce fragmentation of the PAH in any other metal-PAH system studied. The high stability and slow unimolecular dissociation rate of these PAHs do not favor dissociation. Yet, this extended fragmentation exists in both of these spectra. Prominent peaks in both spectra are $Nb_xC_y^+$ and $Nb\text{-}C_xH_y^+$. The most logical explanation for the existence of these peaks is that niobium atoms disrupt the π bonding in these PAHs, becoming strongly bound to or inserted into them during the vaporization process. This is followed by significant rearrangement and dissociation of the ring system resulting in the formation of the carbides and metal-hydrocarbons observed. The early transition metals, niobium included, are known to form carbides with smaller hydrocarbons,[41] but this is the first such result with PAHs.

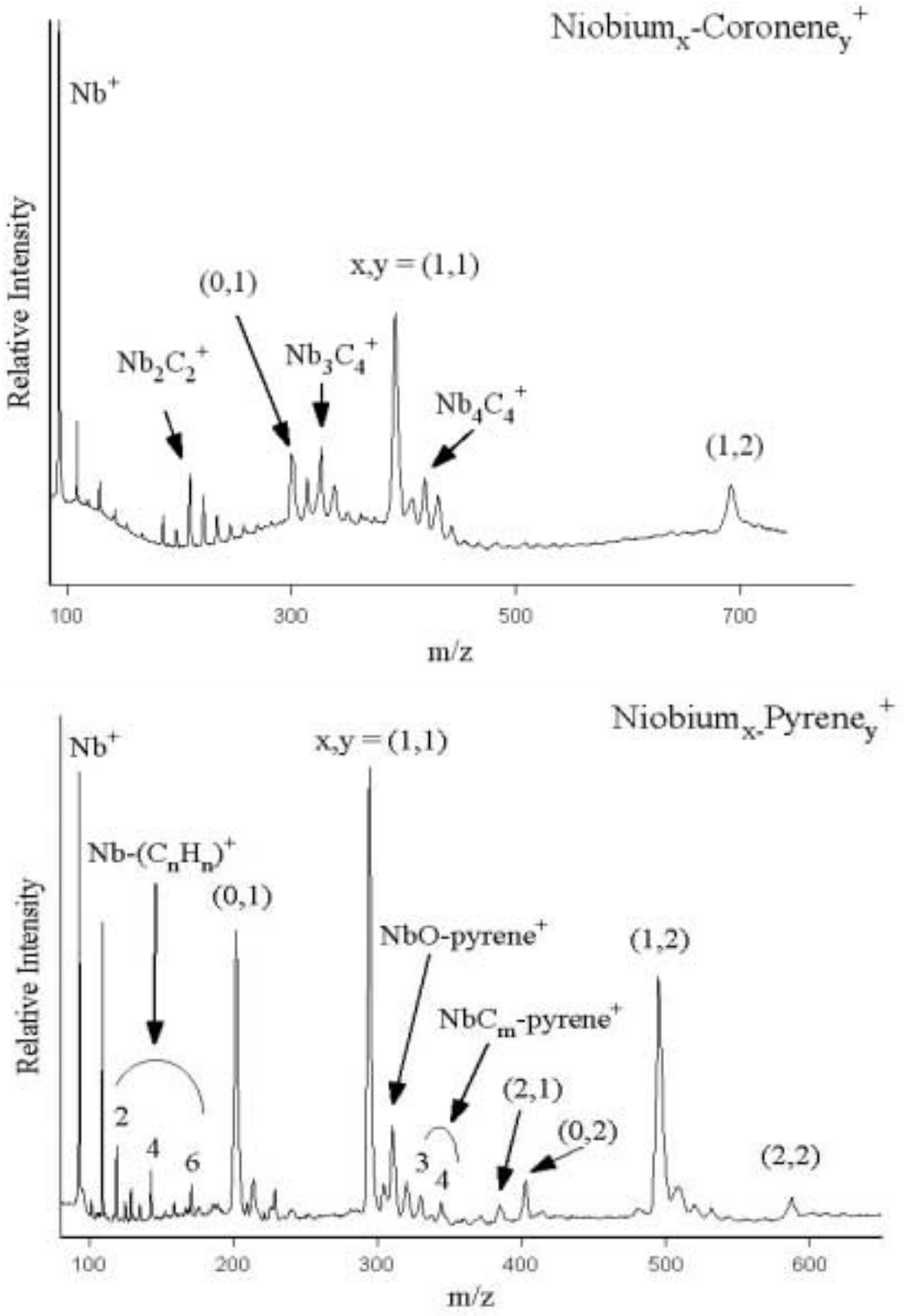

Figure 4-1 : The Mass Spectra of Niobium-Coronene and Niobium-Pyrene.

The obvious preference for single niobium atoms complexes is another new feature. Complexes with two niobium atoms are either not observed (upper trace) or very weak (lower trace). Previous studies with other metals under similar conditions produce M_x-PAH_y^+ up to x = 5 or 6, as illustrated in the previous chapter with chromium. The metal atoms in these systems are thought to cluster together on one side of the PAH molecule or bind to individual binding sites creating a metal film over the PAH surface. Here, the only multi-metal ions observed with any intensity are metal-carbides. The source conditions here are not significantly different than those that produce multi-metal adducts in other systems. The density of metal vapor in this system should be the same as with the other metals. It appears, then, that multiple metal adducts are produced in the plasma, but they must be even more reactive than single metal adducts. These highly reactive multiple metal adducts must dissociate more efficiently than the single metal adducts and bare PAHs to produce some of the multiple metal carbides observed.

Immediately, questions of the mechanism of metal insertion and why niobium is so effective in this type of reaction could be asked. The presence of excited metal atoms in the plasma could certainly promote this kind of insertion. The structures of the resulting metal carbides and metal hydrocarbons are also of interest. Previous ab initio calculations on the metal carbide ions predict a cubic structure as that found in the bulk solid material.[41c]. While there is no direct method to probe the plasma chemistry, some of the structures of the more abundant species can be probed with mass-selected photodissociation. Those findings are presented below.

Figure 4-2 is the photodissociation spectra recorded for Nb-pyrene$^+$ (upper trace) and Nb-pyrene$_2^+$ (lower trace). After an initial loss of molecular hydrogen there is a

systematic loss of $(C_2H_x)_n$ from the parent ion (x = 2 best fits the data, but we do not have unit resolution here). The lower mass fragments show prominent peaks for NbC_4^+ and NbC_6^+. The resolution here is good enough to distinguish between bare carbide and hydrocarbons. It is impossible to tell under these experimental conditions if this systematic fragmentation is concerted, sequential or parallel. The elimination of H_2 and C_2H_x is a known fragmentation channel for isolated PAH ions.[42] Power dependence studies indicate that high laser power is required to observe any fragmentation. Therefore, these fragmentation pathways must be multiphoton which explains how multiple bonds are broken. Additionally, the extent of ring fragmentation is observed to vary with laser power. The sequential loss of C_2H_x eventually producing carbides is consistent with this data. Because hydrogen is depleted before carbon, the carbide masses are an obvious result of such a sequential fragmentation process. These low mass fragments are the same as many of those observed in the initial distribution of cluster masses from the previous mass spectrum for Nb-pyrene. Therefore, it seems that the laser vaporization plasma chemistry is able to fragment the Nb-pyrene system in much the same way as does the photochemistry.

The lower trace shows the same initial loss of H_2 and then a weak series of peaks suggesting the loss of C_2H_x from the parent ion, Nb-pyrene$_2^+$. However, the first prominent peak is Nb-pyrene$^+$. This would result from the loss of an intact pyrene molecule suggesting that in systems with more than one pyrene, the second is not as strongly bound to the niobium atom. The lower mass peaks look almost identical to those in the upper spectra with prominent peaks for NbC_4^+ and NbC_6^+, but with more complete fragmentation of the ring system. While the fragmentation of the upper spectra shows

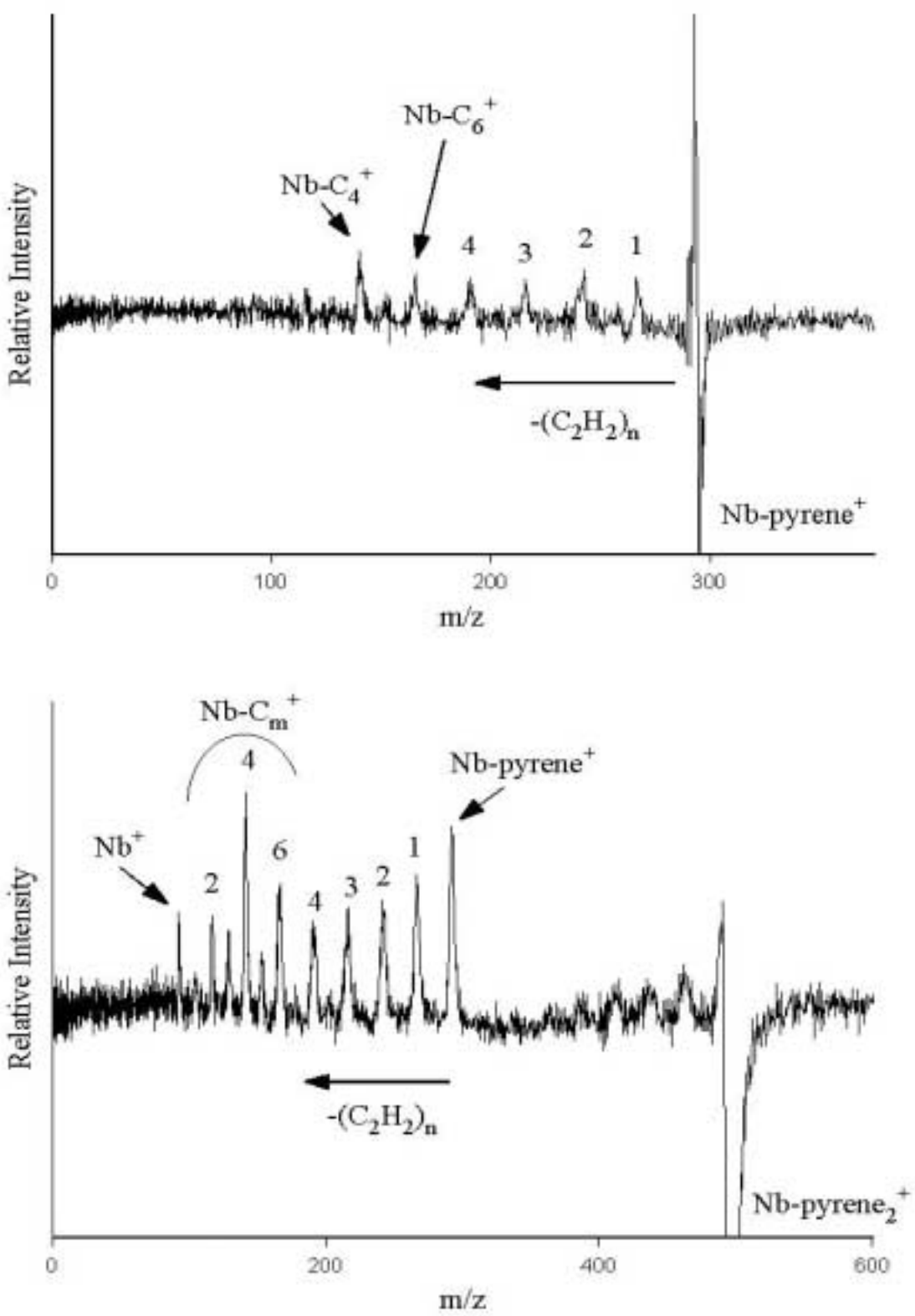

Figure 4-2 : Photodissociation spectra for Niobium-pyrene^{+} and Niobium-pyrene$_2^{+}$.

only these two carbide masses the lower spectra shows all carbide masses down to the bare niobium atom.

Figure 4-3 shows the photodissociation spectra of Nb-coronene$^+$ (upper trace) and Nb-coronene$_2^+$ (lower trace). The fragmentation pattern of the Nb-coronene$^+$ is very similar to that of the Nb-pyrene$^+$. There is the initial loss of molecular hydrogen and then the previously observed sequence indicating loss of C_2H_x, here again, x = 2 best fits the data. In the lower mass region there is a prominent peak for NbC_4^+, as well as all other niobium carbides and the bare niobium ion. The power dependence of these peaks suggests that this is also a sequential dissociation process like in Nb-pyrene$^+$. The lower trace shows that Nb-coronene$_2^+$ fragments in the same manner as Nb-pyrene$_2^+$. The parent ion first loses H_2 and then the next fragment seen is the loss of an intact coronene molecule resulting in Nb-coronene$^+$. The fragmentation pattern is then identical to that of the upper trace with loss of C_2H_2 units down to the carbides and then the atomic ion. Throughout all of these spectra NbC_4^+ has been a prominent fragment ion and it is here as well. The simplest interpretation for this spectrum is that the Nb atom is inserted into one coronene and then weakly binds to another. This second coronene is eliminated efficiently and the resulting complex undergoes a sequence of fragmentation producing the metal-hydrocarbons and metal carbides.

Both the coronene and pyrene systems show similar photodissociation behavior with complete destruction of the ring system. In previous metal-PAH photodissociation studies, conducted on a wide variety of metals, this type of behavior has never been observed. In those studies, single metal complexes where metal = Cr, Fe, Ti, V, Ag, Ni, etc., the photodissociation spectra always showed elimination of metal from an intact ring

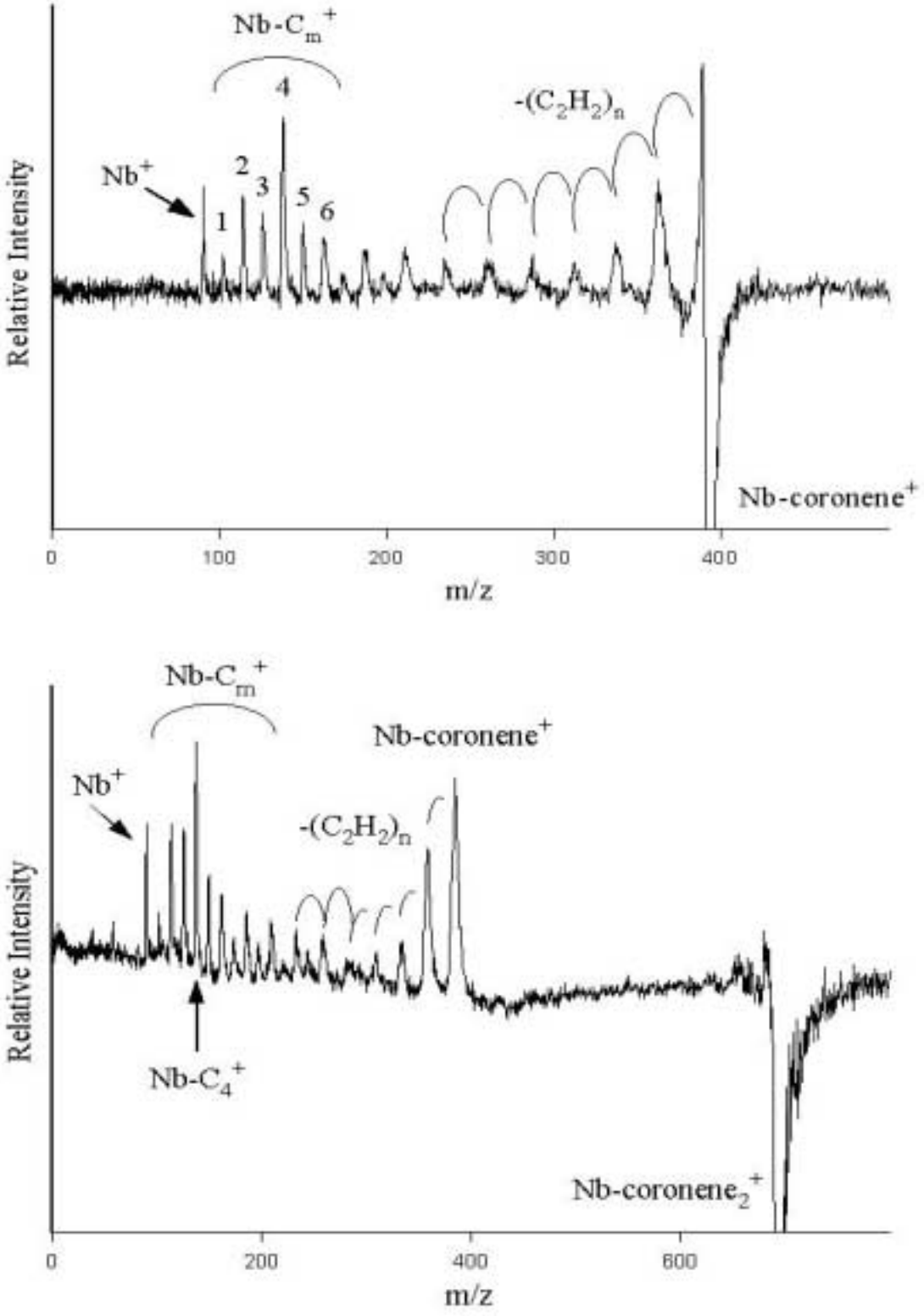

Figure 4 -3 : Photodissociation spectra for Niobium-coronene$^+$ and Niobium-coronene$_2^+$.

system. This study, in which the metal remains intact in a hydrocarbon or carbide structure and the ring dissociates suggests that niobium atom has inserted or become incorporated into the PAH molecule or has caused significant rearrangement of the planar aromatic into a three dimensional metal-hydrocarbon cluster. It is also possible that the Nb-$C_xH_y^+$ masses present in the spectra are actually metallocene intermediates (i.e. Nb-benzene, Nb-napthalene, etc). In previous exohedral metal studies with C_{60}, Martin and coworkers reported that niobium and tantalum were unusual among transition metals in their ability to fracture the fullerene cage.[14] Clusters that contained more than one atom of other metals, such as Ti or V, were also found to react with C_{60} to produce carbides and/or fragments which suggest that they become incorporated into the fullerene wall. Jarrold and coworkers have done ion mobility measurements on Nb-C_{59}^+ that establish that the niobium atom does insert into the fullerene.[43] In that study, niobium and tantalum were reported to be the most reactive. It is apparent that niobium exhibits exceptional chemistry in the presence of PAH ring systems.

This enhanced reactivity is difficult to understand. One could postulate that niobium forms stronger carbides than other transition metals. However, this is not the case. Although it does form one of the most stable bulk carbides, titanium and tantalum have higher carbide bond strengths[44], but neither were found to behave in this manner. It also is conceivable that the metal-arene π bonding strengths are a factor. Although thermochemical measurements for Nb-PAH systems have not been reported, data is available for Nb-benzene.[45] That data shows that niobium does form strong bonds with benzene, but that it is not unusual from other transition metals that also bind strongly. A final possibility and one which is difficult to test, is that niobium atoms and/or cations

that are produced in the laser plasma have a higher concentration of metastable excited states than other metals studied. These excited states are well known to occur in the plasma environment. They also are known to be much more reactive than their ground state counterparts. However, because these metastable metal atoms are known to occur with a number of transition metals, it remains unclear why niobium would be more efficient at accessing these states than other transition metals. Regardless of the mechanism behind it, it is clear that niobium created in laser vaporization experiments exhibits a higher reactivity than any of the other metals we have studied.

CHAPTER 5

SAMARIUM – CYCLOOCTATETRAENE

AND

GADOLINIUM – CYCLOOCTATETRAENE

Shown below are the mass spectra for the lanthanide-cyclooctatetraene (Ln-COT) systems. These cationic complexes are produced first as neutral clusters by laser vaporization of a samarium or gadolinium metal rod (ESPI; grade 3N) with the first harmonic, 532 nm, of an Nd:YAG laser. The cyclooctatetraene, COT, is seeded into the helium carrier gas as explained in the experimental section of this work. A waiting room nozzle extension is utilized. The waiting room is 3 centimeters long with a 1 cm diameter hole covered by a 3 mm exit orifice. The neutral metal-COT complexes are subsequently photoionized with the focused output, 193 nm, of an ArF excimer laser. Both spectra show sequential adducts of metal atoms and organic molecules. Kaya and coworkers have studied similar Ln-COT systems (where Ln = Ce, Nd, Eu, Ho, and Yb) and found them to prefer the (n,n+1) sandwich stoichiometries.[46] In fact, double decker sandwiches of Nd-COT and Ce-COT have been synthesized in the condensed phase.[47] The observation of these types of stoichiometries in the gas phase, where no solvent effects are present, is therefore quite expected. The metals chosen for our study included neodymium, but, unlike Kaya, we opted to study the metals to the right and left of Eu in the periodic table. Because of their proximity, these metals, Sm and Gd, would be expected to exhibit similar behavior. They also provide the study with different oxidation state metals. Samarium has been observed in synthesized Sm-COT complexes to prefer the +2 oxidation state over +3. Gadolinium, on the other hand, has only a +3 oxidation state as does neodymium and lanthanum, the final metal included in the study. Because the information obtained for Gd, Nd, and La was almost identical only one metal is presented here, gadolinium. Another important note about these systems is that these metals have multiple isotopes. This causes broadening of some peaks which contain

more than one metal atom. However, resolution in these spectra is quite good and upon closer inspection many of the individual isotopes can be seen.

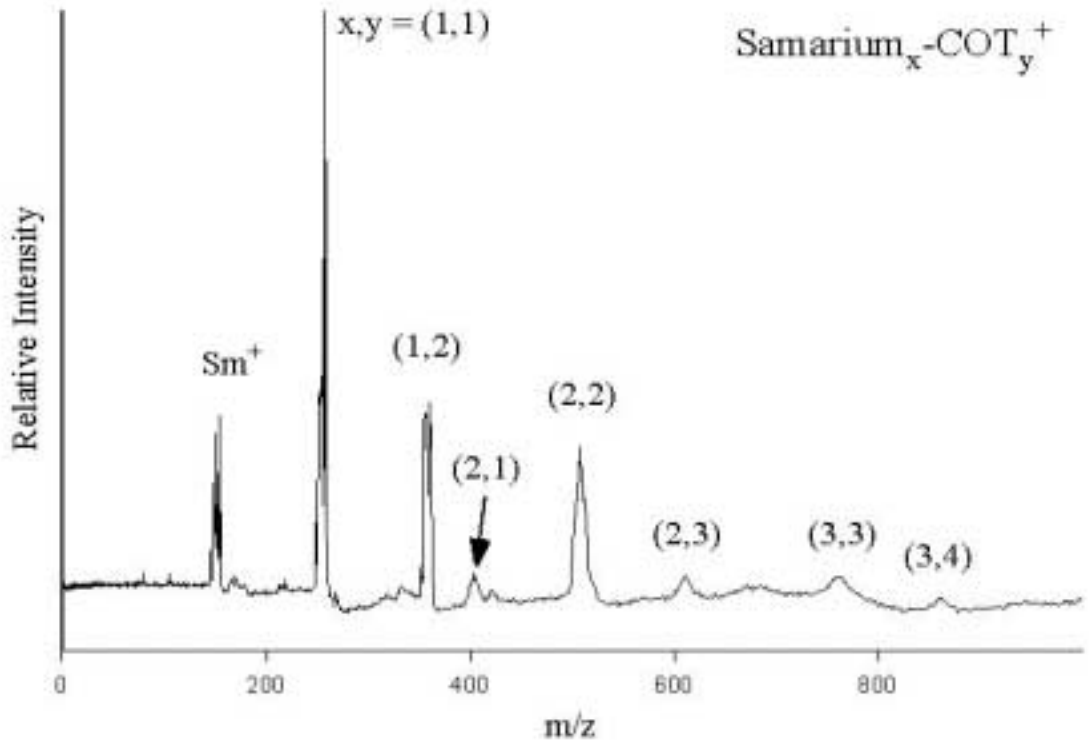

Figure 5-1: Mass Spectrum of Samarium-COT recorded at 355 nm.

In the samarium-COT system, Figure 5-1, there are three series-like progressions each having one more metal atom. The first such progression corresponds to complexes with one metal atom. There is a strong peak at Sm-COT$^+$ in this series followed by a less intense peak for Sm-COT$_2^+$. There are no peaks beyond the (1,2) in this series. The absence of (1,3) or any larger clusters with only one metal suggests that one samarium atom prefers to bind to a maximum of two ligands. The second series is that of the two metal atom complexes. Here there is a weak (2,1) peak followed by an enhanced (2,2) peak. The series then declines sharply showing a weak (2,3) signal. This is the most

complete of the three series. The three metal atom containing complexes are very weak signals. Surprisingly, the first observed cluster is that of (3,3) which is slightly larger than the (3,4). The notable absence of (3,1) and (3,2) suggests that these complexes are not comprised of metal atoms clustered on the surface of COT, as was the case in some of the Cr-coronene complexes. This is in agreement with the fact that clusters beyond the samarium dimer were not observed to be produced under these source conditions without the presence of COT. These complexes must then be formed not randomly, but with some ordered structure. Overall, this spectrum suggests that samarium prefers a (n,n) type stoichiometry over the (n,n+1) stoichiometry usually observed for sandwiches. However, as previously stated, in condensed phase chemistry, samarium is known to form sandwiches. A reasonable explanation for this behavior is found in the two possible oxidation states, +2 and +3. The organic ligand, COT, is most stable as a dianion. This causes the molecule to become planar and obey the 4n+2 rule of aromaticity. It is then easy to understand why the (1,1) is the most stable conformation for the neutral complexes created in the source as one samarium would donate two electrons to COT creating a stable, neutral, ionicly bonded complex. This is consistent with the fact that samarium has been reported to prefer the +2 oxidation state in the synthetically prepared half-sandwich complex and also that Sm-COT complexes are reported to be polymeric.[48] The structure of the (n,n) stoichiometries is therefore an interesting question. They could exist as sandwiched dimers or they also could be sandwiches with uncapped metal atoms, or, in the case of larger multimers, as ligand-coated metal clusters. We have employed mass-selected photodissociation experiments to provide more information. Figure 5-2 shows the photodissociation of Sm-COT (upper trace) and Sm-COT_2^+ (lower trace).These clusters were photoexcited with the focused output, 355 nm, of a Nd:YAG laser.

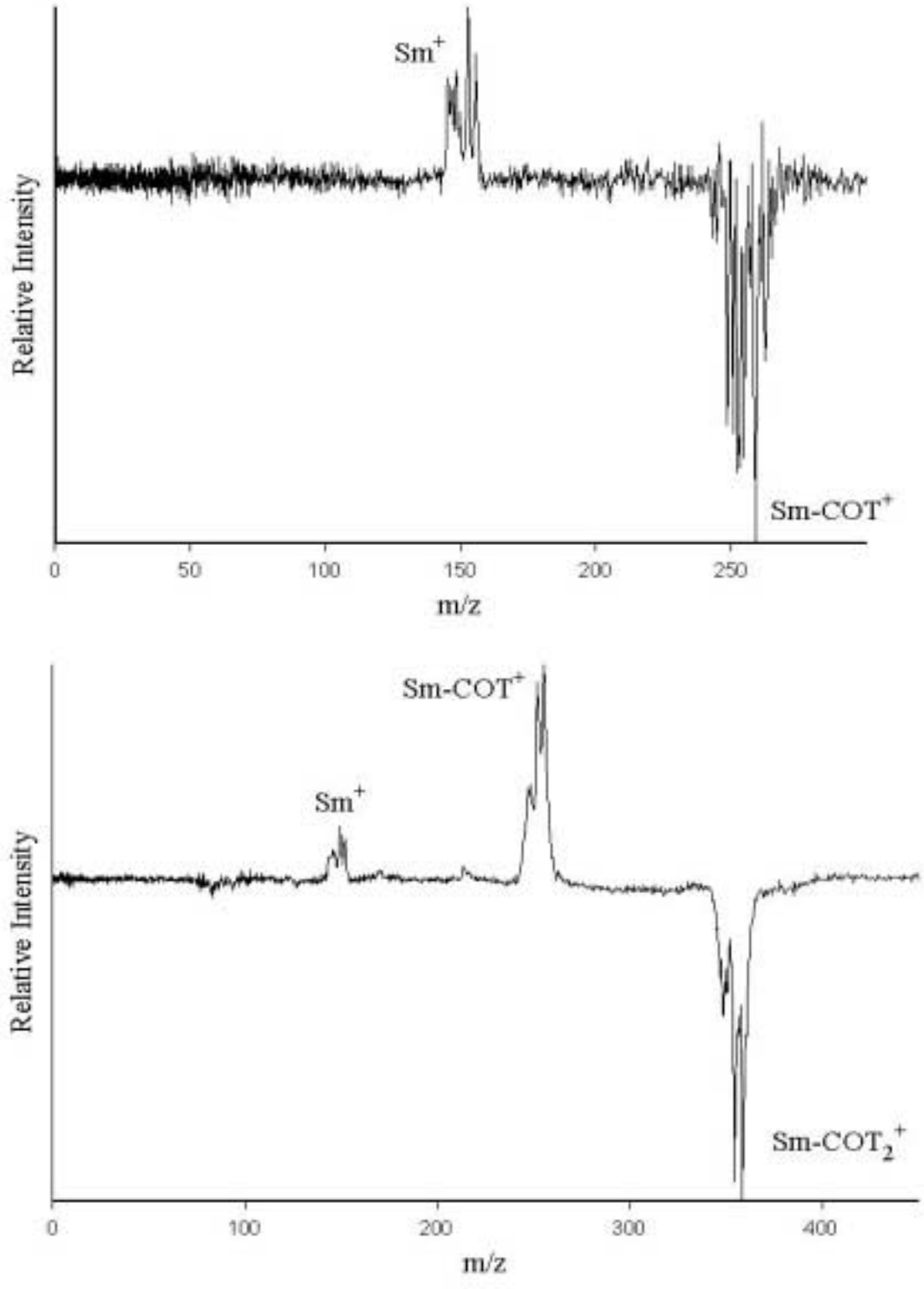

Figure 5-2: The photodissociation mass spectra of Samarium-COT^+

and Samarium-COT_2^+ at 355 nm.

Although laser intensity was varied to observe any change in the fragmentation pattern, it did not cause significant deviation from what is observed here. The ionization potential (IP) of Sm is 5.6437 eV [49] and that of COT is 8.0 eV. [49] The expected result of photodissociation would be simple cleavage of the metal-ligand bond resulting in Sm^+. Indeed, the upper trace shows the expected metal elimination as the only fragmentation channel. The lower spectrum shows loss of an intact COT resulting in Sm-COT^+ suggesting that Sm-COT^+ has an IP lower than that of COT. Further fragmentation of this complex leads to the bare Sm^+. This is similar behavior to the analogous Cr-coronene$^+$ discussed in Chapter 2. Most of the novel organometallics we have studied exhibit these same fragmentation pathways.

The photodissociation spectra of the multiple metal complexes is shown in Figure 5-3. Sm_2-COT has been observed in solution phase chemistry to be an inverted sandwich with samarium molecules on either side of the COT molecule.[48] However, the fragments observed in this spectrum suggest that the metal is clustered together or at the very least the interaction between the two is great enough to keep them together through the fragmentation process. This is evident in the markedly different fragmentation pattern shown here indicating dissociation of the COT ring system. The upper trace, Sm_2-COT^+, shows an initial loss of consecutive C_2H_2 units. This results in a prominent Sm_2-$C_4H_4^+$ peak along with less intense Sm_2-$C_6H_6^+$ and Sm_2-$C_2H_2^+$ peaks. Another new feature is the presence of Sm-$C_2H_2^+$ which must result from the further fragmentation of the Sm_2-$C_4H_4^+$or directly from the parent ion since it was not observed as a fragment of Sm-COT^+. The previously observed Sm-COT^+ and Sm^+ fragments are present here as well. The presence of Sm-COT^+ indicates that it not only has an IP lower than that of COT, but

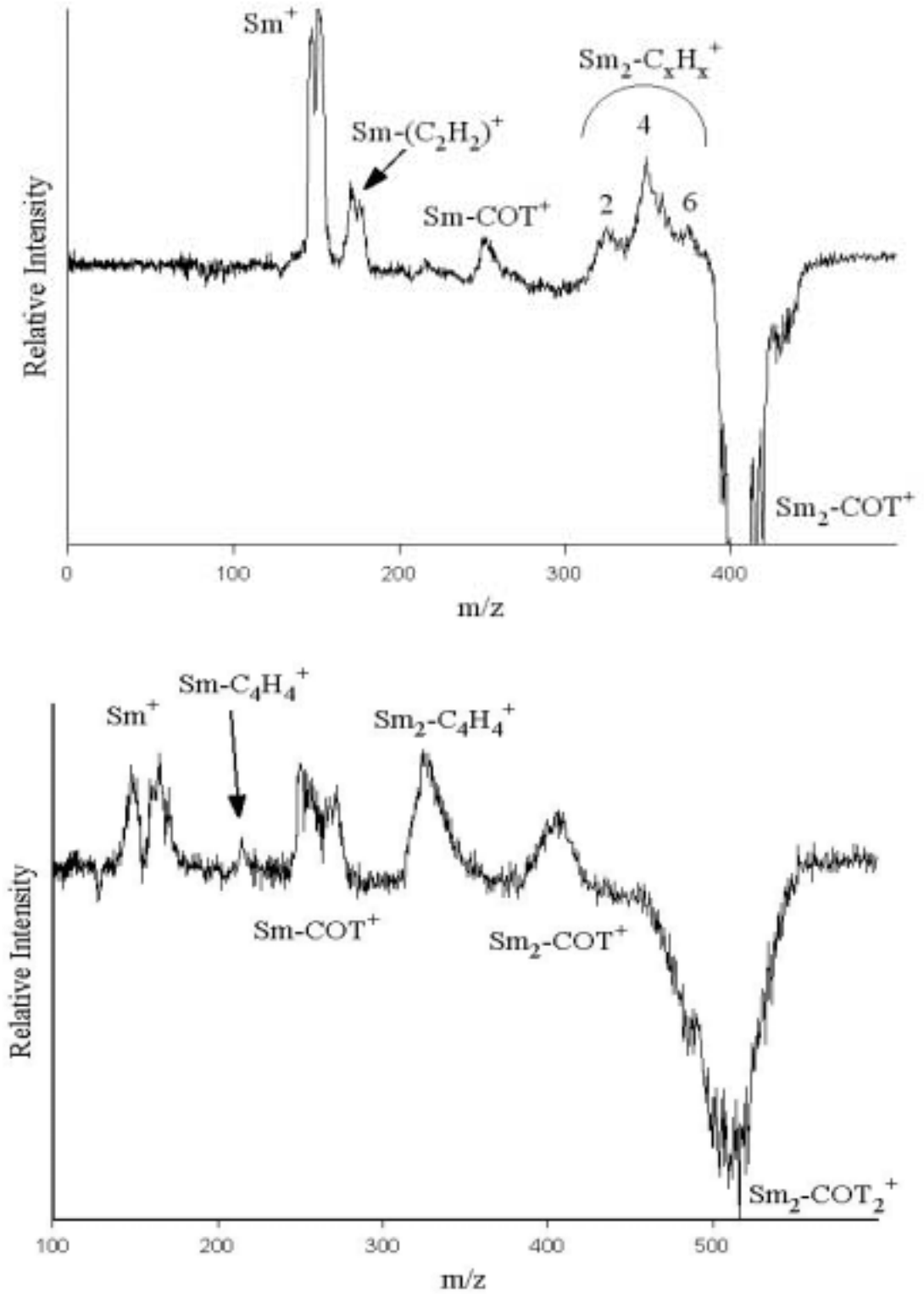

Figure 5-3: The photodissociation mass spectra of

Samarium$_2$-COT$^+$ and Samarium$_2$-COT$_2^+$ at 355 nm.

also of Sm, as Sm_2-COT^+ would have to lose a neutral Sm atom in order for this to be produced. The mass spectrum of COT alone,[45] not shown here, shows that the most prominent fragment ion is $C_6H_6^+$ and while that fragment is observed here it is not the most prominent. Because samarium is suspected to bond to opposite sides of the COT ring and the ring strain of cyclobutene is very high, it is unlikely that the Sm_2-$C_4H_4^+$ is a four membered ring sandwiched by two metal atoms. It is more likely to be an open ring fragment with Sm atoms at each end. This would also account for the splitting fragment, Sm-$C_2H_2^+$ because the larger cluster would have the samarium atoms separated by a single C – C bond :

$$\begin{array}{cccc} Sm & & Sm & \\ C = C & - & C = C & \end{array}$$

The fragmentation of that single C – C bond would result in two Sm-$C_2H_2^+$ molecules.

This extended fragmentation is observed again in the lower trace of Sm_2-COT_2^+. Apart from the initial loss of an intact COT molecule from the parent ion this spectrum is very similar to the upper trace. There is a prominent Sm_2-$C_4H_4^+$ signal along with the Sm-COT^+ and Sm^+ as seen above. However, instead of Sm-$C_2H_2^+$ we observe Sm-$C_4H_4^+$. These peaks suggest that although the samarium atoms are strongly bound to one cyclooctatetraene molecule, the second COT is weakly attached and dissociates efficiently. Although these studies do not provide conclusive structural determinations it is of interest to note that it takes two samarium molecules to cause ring fragmentation of the COT molecule and that even in the multiple COT complexes those fragmentation pathways remain relatively the same.

The mass spectrum of Gd-COT is shown in Figure 5-4. Here we observe only two series, the single metal and double metal atom complexes. The strong intensity of

the gadolinium ion signal, which has been omitted here to show the rest of the spectrum in greater detail, suggests that although there is an abundance of gadolinium available to react with itself in the source it does not readily do so. Gadolinium was observed not to cluster beyond the dimer in these source conditions. Within the first series of single metal

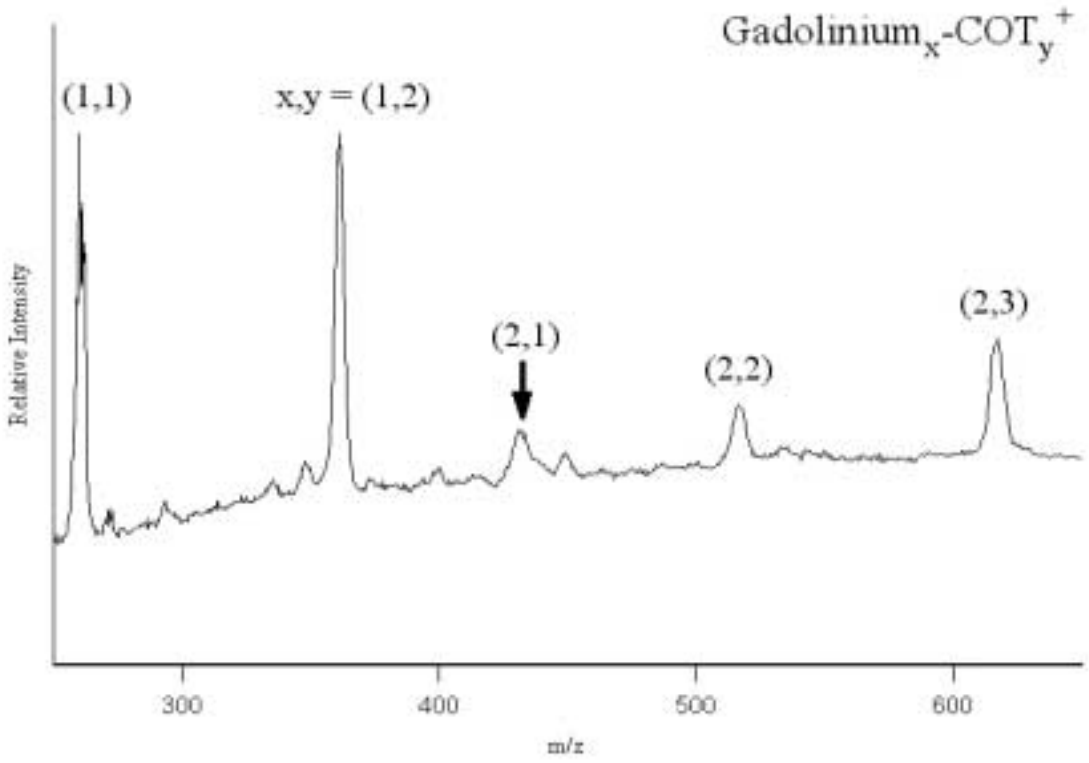

Figure 5-4: The Mass Spectrum of Gadolinium-cyclooctatetraene.

atom complexes there is again only the (1,1) and (1,2) and they are of equal intensity. Gadolinium, like samarium, is known to produce sandwich complexes in solvent stabilized solution phase experiments.[24] However, gadolinium possesses only one oxidation state, +3. This may explain the lack of cluster signal provided the abundance of gadolinium atoms. In the double atom series the (2,1), (2,2) and (2,3) are observed as seen previously with the Sm-COT system. However, here the enhanced signal is the

(2,3). This is best understood by considering the oxidation state of the metal and remembering that the ions photodissociated here were initially neutral species in the source. The most natural neutral molecule created by the interaction of Gd (+3) with COT (-2) would be Gd_2-COT_3. This stoichiometry, as mentioned before, has been previously reported by Kaya and coworkers in their work with lanthanide-COT systems in the gas phase[46] and by Edelman in his condensed phase work with these lanthocenes[48]. It is believed to be the double decker sandwich structure. Mass selected photodissociation studies provide the following information.

Figure 5-5 is the photodissociation spectra of Gd-COT^+ (upper trace) and Gd-COT_2^+ (lower trace). Since the IP of gadolinium (6.15 eV)[49] is lower than that of COT (8.0 eV) the expected fragmentation is simple elimination of gadolinium cation. That is observed, however, it is not a clean elimination as in the samarium complexes. In fact, the fragmentation of Gd-COT^+ differs from that of Sm-COT^+ significantly. It is obvious here that only one gadolinium atom is necessary to cause fragmentation and Gd-$C_5H_5^+$ is the most prominent fragment ion. This holds throughout the laser power dependence studies and increases in intensity with increasing laser power. There is also a small peak indicating the presence of Gd-$C_6H_6^+$. This peak remains stable in intensity under a variety of laser fluences. The observation of immediate ring fragmentation is consistent with a strong ionic interaction. This is also consistent with Kaya's report of a stronger binding energy in systems with +3 oxidation state metals.[10]

The lower trace of Gd-COT_2^+ shows the only high mass peak is Gd-COT^+ which results from loss of an intact COT molecule. The low mass fragments are identical to that of the upper spectrum. Therefore, it appears that the second COT molecule is only weakly

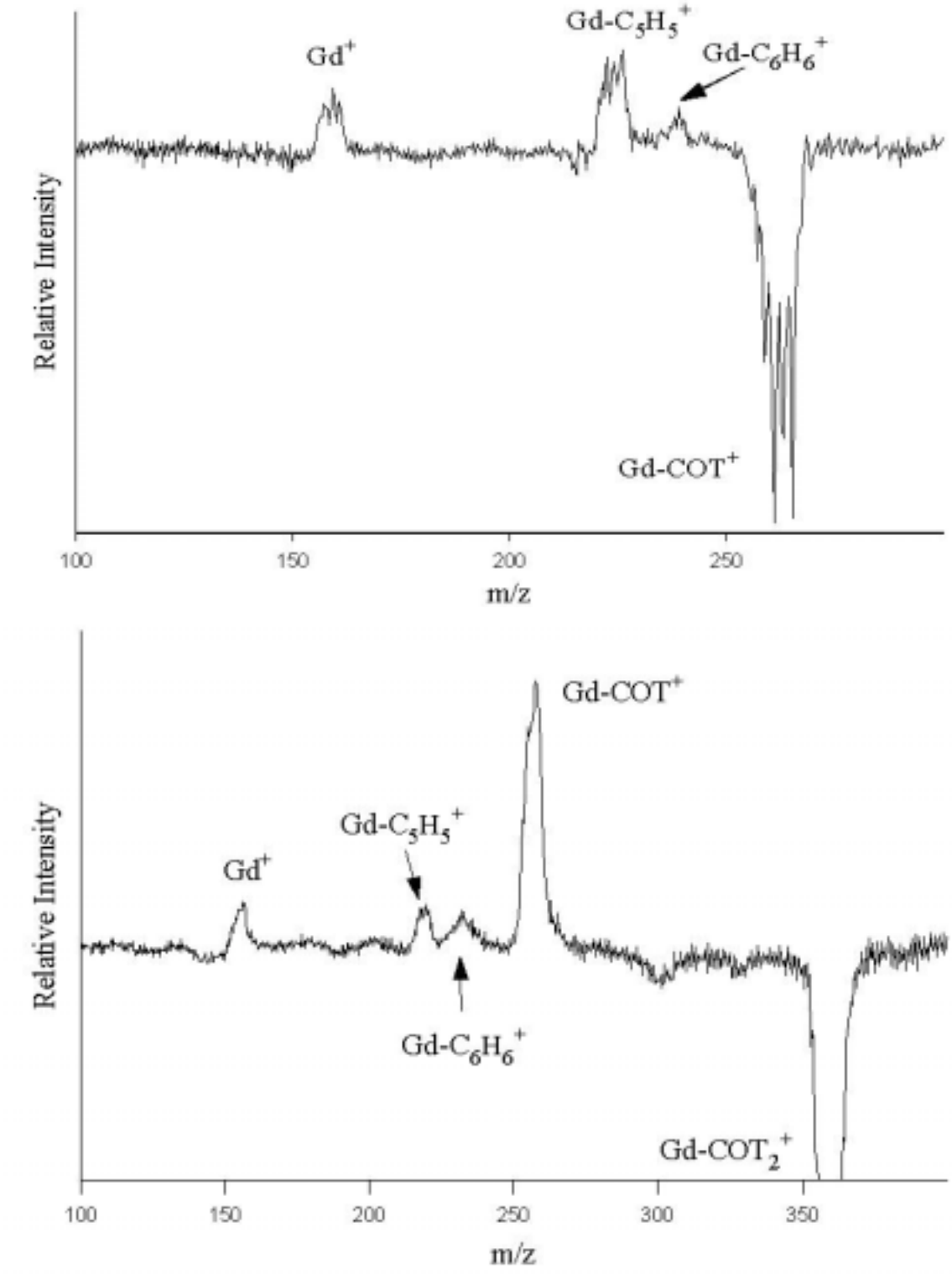

Figure 5-5: Photodissociation Spectra of Gadolinium-COT^+

and Gadolinium-COT_2^+ at 355 nm.

interacting with the gadolinium atom as in Sm_2-COT_2^+ and as in the Nb-PAH systems discussed in the previous chapter.

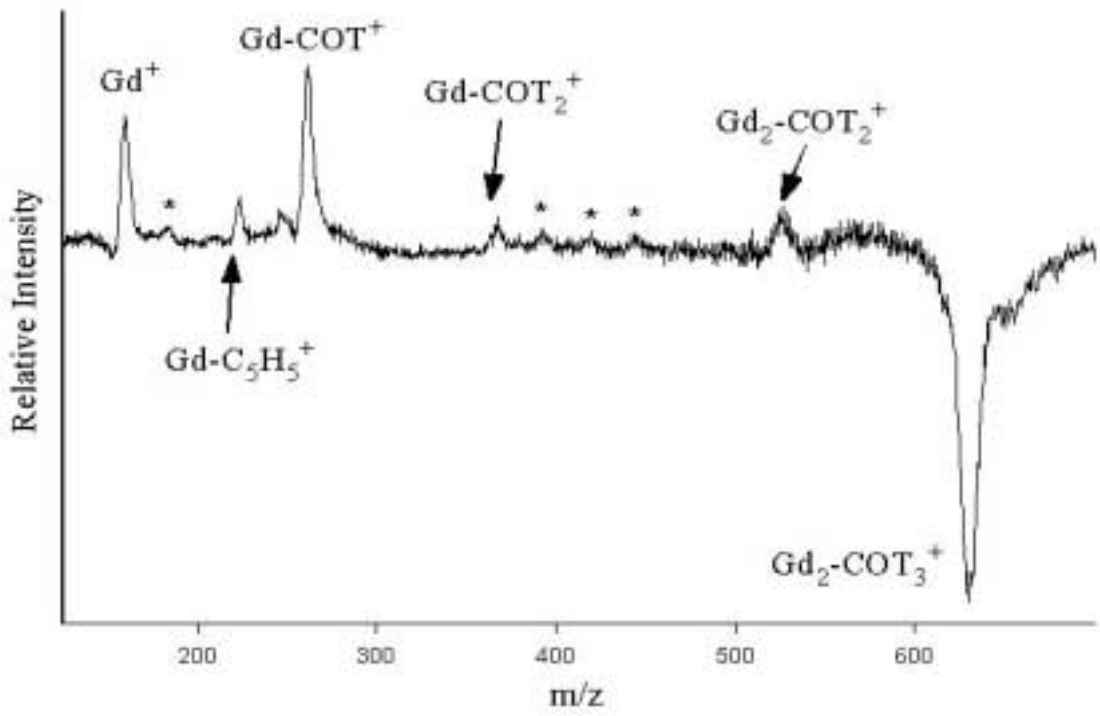

Figure 5-6: Photodissociation Mass Spectrum of Gadolinium$_2$-COT_3^+ at 355 nm.

The photodissociation spectrum of Gd_2-COT_3^+ is shown in Figure 5-6. This is the highest mass cluster observed in the original distribution of clusters photoionized from the source. Relatively high laser power was necessary to observe any fragmentation indicating that this is a reasonably stable molecule. This inherent stability is consistent with the argument that the (2,3) would be the most likely neutral produced under the source conditions. The most prominent features in the spectra are Gd^+ and Gd-COT^+ similar to what was observed in the previous spectrum. However, a number of new features are present. There are the expected intact metal-ligand clusters of Gd-COT_2^+ and

Gd_2-COT_2^+ which were observed in the original mass spectrum and would be the result of loss of a metal atom or intact COT molecule, respectively. However, between these two peaks are three peaks marked with an asterisk. These peaks cannot be identified as complexes containing whole COT molecules and due to the difficulty created by mass coincidences they cannot be identified with certainty. Three possibilities exist for these unassigned peaks. The first possibility is that these represent a Gd-COT_2-$C_nH_n^+$ progression, where n = 2, 4, and 6. The (1,2) is observed in the source to be a stable molecule and COT is known to fragment into $C_6H_6^+$ and to a lesser degree other $C_nH_n^+$ fragments. The second possibility is that these peaks represent, from left to right, Gd_2-$C_6H_6^+$, Gd_2-COT^+, Gd_2-COT-$C_2H_2^+$. This is also a plausible explanation based on the clusters observed in the initial cluster distribution. The (2,1) signal is weak, as are these peaks indicating that they are not stable and would be more likely to dissociate in the environment of the photoexcitation laser. The third possibility is that these clusters represent some combination of the two. The small peak to the right of the Gd^+ can be assigned as Gd-$C_2H_2^+$, although the broadening of the peaks in this spectrum makes unit resolution unattainable. This would be consistent with the first and third asterisked peaks being Gd-COT_2-$C_2H_2^+$ and Gd_2-COT-$C_2H_2^+$, whereas the middle peak is most likely the (2,1). Regardless of what these peak actually are, the interesting thing about them is that here complexes do not always adopt an odd numbered hydrocarbon fragment from the COT. Previous spectra show the prominent COT fragmentation as C_5H_5 and it is somewhat unexpected that the higher mass fragmentation does not follow this pattern.

The fragments observed are consistent with a sandwich structure if only the peaks with greatest intensity are considered. A sandwich would fragment sequentially, first

ejecting neutral COT, then Sm, then COT and finally the last COT leaving Sm^+. That is exactly what is shown here to be the predominant fragmentation pathway.

CHAPTER 6

CONCLUSIONS

These studies have provided evidence that laser ablation of a coated rod or clean rod with seeded carrier gas can effectively and easily produce gas phase organometallic complexes. The ability to mimic the interstellar environment provides an opportunity to study clusters which may have some significance in the effort to assign the UIRs and DIBs that currently have no known cause.

It has also been shown that these complexes have distinct dissociation pathways. Although our lab has investigated many transition metal – PAH complexes and observed a regular pattern of dissociation the complexes presented here do not follow that pattern. Most metal-coronene complexes dissociate readily into whole subunits of M-ligand. Chromium-coronene shows similar behavior to those previous results until a required number of metal atoms per coronene molecule is obtained. At Cr_4-coronene$^+$ the metal cluster begins to cause disruption of the coronene ring system resulting in masses which can only be assigned as Cr_x-$C_nH_n^+$ where the hydrocarbon fragment is benzene, napthalene or pyrene.

A more impressive example of ring destruction is observed with niobium-coronene and niobium-pyrene. In these systems only one metal atom is necessary to reduce the coronene ring to hydrocarbon and metal carbide fragments. Niobium is also unique in that it prefers single metal complexes. However, carbide fragments are observed for Nb_x-C_y up to $x = 4$ in the original source distribution of clusters suggesting that higher mass clusters are immediately reduced to metal carbides as they are created. These higher mass niobium carbides do not form during photodissociation indicating that these are not merely rearrangements or clusters of existing Nb-C fragments.

The lanthanide-COT systems provide evidence for ring disruption of a nonaromatic organic ligand in the presence of metal. Although with the donation of

electrons from the metal to the COT the 4n+2 rule of aromaticity is obtained. Here information supporting previous reports of stronger binding in systems that contain a metal with a +3 oxidation state, here gadolinium, over than of systems with a +2 metal, here samarium, is observed. It is also shown that multiple samarium atom complexes do bind strongly enough to cause ring fragmentation upon photodissociation.

Future studies should focus on lanthanide metal interactions with various hydrocarbon molecules, such as coronene. Because these metals have very little covalent character, they may produce interesting structural patterns. Other possibilities are to attempt to synthesize the Ln-COTs via our laser vaporization flow tube reactor (LVFR). Since the basic building blocks of Ln-COT sandwiches are known to exist in solution this system represents a unique opportunity to create larger sandwiches which can be isolated for structural characterization.

Although the metal-PAH systems have been studied in depth in our laboratory these systems still hold promise for providing further information on the relative binding strengths of many metal-arene systems. More competitive binding studies would certainly yield interesting and necessary information on the energetics of the metal-organic ligand interaction.

BIBLIOGRAPHY

Afzaal, S.; Freiser, B.S. *Chem. Phys. Lett.*, **1994**, *218*, 254.

Allamandola, L.J.; Tielens, A.G.G.M.; Barker, J.R.; *Astrophys. J.*, **1985**, *290*, L25.

Armentrout, P.B.; Hales, D.A.; Lian, L., *Adv. Metal & Semiconductor Clusters*, M.A. Duncan, ed., **1994**, Vol. 2, p.1 (JAI Press, Greenwich, CT).

Bauschlicher, C.W.; Partridge, H.; S.R. Langhoff, *J. Phys. Chem*., **1992**, *96*, 3273.

Bauschlicher, C.W.; Partridge, H.; S.R. Langhoff, *J. Phys. Chem*., **1992**, *96*, 3273.

Branz, W.; Billas, I.M.L.; Malinowski, N.; Tast, F.; Heinebrodt, M.; Martin, T.P. *J. Chem. Phys.*, **1998**, *109*, 3425.

Buchanan JW, Grieves GA, Flynn ND, Duncan, M.A. *Intl. J. Mass. Spectrom*.,**1999**, *187*, 617.

Buchanan JW; Reddic JE, Grieves GA, Duncan, M.A, *J. Phys. Chem.* **1998**, *102*, 6390.

Buchanan, J.W.; Grieves, G.A.; Reddic, J.E.; Duncan, M.A., *Intl. J. Mass. Spectrom*., **1999**, *182*, 323

Buchanan, J.W.; Reddic , J.E.; Grieves, G.A.; Duncan, M.A.; *J. Phys. Chem., A* **1998**, *102*, 6390.

Chaudret, B.; Le Beuze, A.; Rabaâ, H.; Saillard, J.Y.; Serra, G., *New J. Chem*. **1991**, *15*, 791.

Chen, Y.M.; Armentrout, P.B. *Chem. Phys. Lett*., **1993**, *210*, 123.

Clemmer, D.E.; Hunter, J.M.; Shelimov, K.B.; Jarrold, M.F. *Nature (London),* **1994**, *372*, 248.

Clemmer, D.E.; Hunter, J.M.; Shelimov, K.B.; Jarrold, M.F., *Nature* **1994**, *372*, 248.

Cottrell, *Chemical Bonding in Transition Metal Carbides*, The Institute of Materials, London, **1995**.

DeKock, C.W.; Ely, S.R.; Hopkins, T.E.; Bault, M.A. *Inorg. Chem.*, **1988**, *17*, 625.

Dietz, T.G.; Duncan, M.A.; Powers, D.E.; Smalley, R.E:, *J. Chem. Phys*., **1981**, **74**, 6511.

Duncan, M.A., *Ann. Rev. Phys. Chem.*, **1997**, *48*, 63.

Edelmann, F.T. *New J. Chem* **1995**, *19*, 535.

Ely, S.R.; Hopkins, T.E.; DeKock, C.W. *J. Am. Chem. Soc.* **1976**, *98*, 1624.

Fischer, E.O.; Hafner, W. *Z. Naturforsch B.*, **1955**, *10*, 665.

Foster, N.R.; Buchanan, J.W.; Flynn, N.D.; Duncan, M.A. *Chem. Phys. Lett.*, **2001**, *341*, 476.

Foster, N.R.; Grieves, G.A.; Buchanan, J.W.; Flynn, N.D.; Duncan, M.A. *J. Phys. Chem. A.*, **2000**, *104*, 11055.

Freiser, B.S. *Chemtracts Anal Phys*, **1989**, *1*, 65.

Fye, J.L.; Jarrold, M.F., *Intl. J. Mass Spec*. ,**1999**, *187*, 507.

Fye, J.L.; Jarrold, M.F., *Intl. J. Mass Spec*. ,**1999**, *187*, 507.

Gord, J.R.; Freiser, B.S**.**, Buckner, S.W. *J. Phys. Chem.*, **1991**, *95*, 8274.

Greco, A.; Cesca, S.;Bertolini, G. *J. Org. Chem*., **1976**, *113*, 321.

Hayes, R.G.; Thomas, J.L. *J. Am. Chem. Soc.*, **1969**, *120*, 1891

Heck, R.F., *Organotransition Metal Chemistry, A Mechanistic Approach*; Academic Press: New York, **1974**.

Hodgson, K.O.; Mares, F.; Starks, D.F.; Streitwieser, A. Jr. *J. Am. Chem. Soc.*, **1973**, *95*, 8650.

Hoshino, K.; Kurikawa, T.; Takeda, H.; Nakajima, A.; Kaya, K., *J. Phys. Chem.* **1995**, *99*, 3053.

Judai, K.; Hirano, M.; Kawamata, H.; Yabushita, S.; Nakajima, A.; Kaya, K., *Chemical Physics Lett*.**1997**, *270*, 23.

Kealy, T.J.; Pauson, P.L. *Nature* **1951**, *168*, 1039

Kinsley, S.A.; Streitwieser, A., Jr.; Zalkin, A. *Organometallics*, **1985**, *4*, 52.

Klotz, A.; Marty, P.; Boissel, P.; de Caro, D.; Serra, G.; Mascetti, J.; de Parseval, P.; Deroualt, J.; Daudey, J. P.; Chaudret, B., *Planet. Space Sci.* **1996**, *44*, 957.

Klotz, P. Marty, P. Boissel, G. Serra, B. Chaudret, and J.P. Daudey. *Astron. Astrophys.* **1995**, *304*, 520.

Kroto, H.W.; Heath, J.R.; O'Brien, S.cc.; Curl, R.F.; Smalley, R.E. *Nature (London)*, **1985**, *318*, 162.

Kurikawa, T.; Nagao, S.; Miyajima, K.; Nakajima, A.; Kaya, K., *J. Phys. Chem. A* **1998**, *102*, 1743.

Kurikawa, T.; Negishi, Y.; Hayakawa, F.; Nagao, S.; Miyajima, K.; Nakajima, A.; Kaya, K. *J. Am. Chem. Soc*., **1998**, *120*, 11766.

Lias, S.G. "Ionization Energy Evaluation" in NIST Chemistry WebBook, NIST Standard Reference Database Number 69, Eds. W.G. Mallard and P.J. Linstrom, February 2000, National Institute of Standards and Technology, Gaithersburg MD, 20899 (http://webbook.nist.gov).

Martin, T.P.; Malinowski, N.; Zimmerman, U.; Naher, U.; Schaber, H.J., *J. Chem. Phys.* **1993**, *99*, 4210.

Meyer, F.; Khan, F.A.; Armentrout, P.B. *J. Am. Chem. Soc*., **1995**, *117*, 9740.

Morrison, W.H.; Ho, E.Y.; Hendrickson, D.N., *Inorg. Chem*. **1975**, *14*, 500.

Nakajima, A.; Nagao, S.; Takeda, H.; Kurikawa, T.; Kaya, K., *J. Chem. Phys.* **1997**, 107, 6491.

Nagao, S.; Kurikawa, T.; Miyajima, K.; Nakajima, A.; Kaya, K., *J. Phys. Chem. A* **1998**, **102**, 4495.

Nagao, S.; Negishi, Y.; Kato, A.; Nakamura, A.; Nakajima, A.; Kaya, K., *J. Phys. Chem. A* **1999**, *103*, 8909.

Nakajima, A.; Kaya, K., *J. Phys. Chem. A* **2000**, *104*, 176.

Pilgrim, J.S.; Brock L.R.; Duncan, M.A., *J. Phys. Chem.*, **1995**, *99*, 544.

Pozniak, B.P.; Dunbar, R.C. *J. Am. Chem. Soc.* **1997**, *119*, 10439.

Reddic, J.E.; Robinson, J.C.; Duncan, M.A. *Chem. Phys. Lett.*, **1997**, *279*, 203.

Simard, B.; Lebeault-Dorget, M.-A.; Marijnissen, A.; ter Meulen, J.J., *J. Chem. Phys.* **1998**, *108*, 9668.

Schmitt, G.;. Kein, WS.; Fleischhauer, J.; Walbergs, U., *J. Organomet. Chem*. **1978**, *152*, 315.

Tast, F.; Malinowski, N.; Billas, I.M.L.; Heinebrot, M.; Martin, T.P., *Z. Phys. D: At., Mol. & Clusters*, **1997**, *40*, 351.

Tast, F.; Malinowski, N.; Frank, S.; Heinebrot, M.; Billas, I.M.L.; Martin, T.P., *Phys. Rev. Lett.* **1996**, *77*, 3529.

Thayer, J.S., *Organometallic Chemistry, An Overview*; VCH publishers, Inc.: New York, 1988.

Wang, X.; Becker, H.; Hopkinson, A.C.; March, R.E.; Scott L.T.; Bohme, D.K., *Intl. J. Mass Spec.*, **1997**, *161*, 69.

Wei, S.; Guo, B.C; Deng, H.T.; Kerns, K.; Purnell, J.; Buzza, S.A.; Castlemann, Jr. A.W., *J. Am. Chem. Soc*., **1994**, *116*, 4475.

Weis, P.; Kemper, P.R.; Bowers, M. *J. Phys. Chem*. **1997**, *104*, 8207.

Streitwieser Jr., A; Müller-Westerhoff, U. *J. Am. Chem. Soc.*, **1968**, *90*, 7364.

Wiley, W.C. and McLaren, I.H., *Rev. Sci. Instrum.*, **1955**, *26*, 1150.

Wiley, K.F.; Cheng, P.Y.; Bishop, M.B.; Duncan, M.A. *J. Am. Chem. Soc*. **1991**, *113*, 4721.

Willey, K.F.; Cheng, P.Y.; Pearce, K.D.; Duncan, M.A. *J. Phys. Chem.*, **1990**, *94*, 4769.

Willey, K.F.; Yeh, C.S.; Robins, D.L.; Duncan, M.A. *J. Phys. Chem.*, **1992**, *96*, 9106.

Yeh, C.S, Byun, Y.G.; Afzaal, S.; Kan, S.Z.; Lee, S.; Freiser, B.S.; Hay, P.J., *J. Am. Chem. Soc*., **1995**, *117*, 4042

Yeh, C.S.; Pilgrim, J.S.; Robbins, D.L.; Willey, K.F.; Duncan, M.A., *Intl. Rev. Phys. Chem.* **1994**, *13*, 231.

Zimmerman, U.; Malinowski, N.; Naher, U.; Frank, S.; Martin, T.P., *Phys. Rev. Lett*. **1994**, *72*, 3542.

WORKS CITED

[1] Thayer, J.S., *Organometallic Chemistry, An Overview*; VCH publishers, Inc.: New York, **1988**.

[2] Heck, R.F., *Organotransition Metal Chemistry, A Mechanistic Approach*; Academic Press: New York, **1974**.

[3] Kealy, T.J.; Pauson, P.L. *Nature* **1951**, *168*, 1039

[4] Fischer, E.O.; Hafner, W. *Z. Naturforsch B.*, **1955**, *10*, 665.

[5] a) Afzaal, S.; Freiser, B.S. *Chem. Phys. Lett.*, **1994**, *218*, 254. b) Gord, J.R.; Freiser, B.S., Buckner, S.W. *J. Phys. Chem.*, **1991**, *95*, 8274. c) Freiser, B.S. *Chemtracts Anal Phys*, **1989**, *1*, 65.

[6] Bauschlicher, C.W.; Partridge, H.; S.R. Langhoff, *J. Phys. Chem*., **1992**, *96*, 3273.

[7] a) Wiley, K.F.; Cheng, P.Y.; Pearce, K.D.; Duncan, M.A. *J. Phys. Chem*. **1990**, *94*, 4769. b) Wiley, K.F.; Cheng, P.Y.; Bishop, M.B.; Duncan, M.A. *J. Am. Chem. Soc*. **1991**, *113*, 4721. c) Wiley, K.F.; Yeh, C.S.; Robins, D.L.; Duncan, M.A. *J. Phys. Chem.*, **1992**, *96*, 9106.

[8] a) Willey, K.F.; Yeh, C.S.; Robins, D.L.; Duncan, M.A. *J. Phys. Chem.*, **1992**, *96*, 9106. b) Willey, K.F.; Cheng, P.Y.; Pearce, K.D.; Duncan, M.A. *J. Phys. Chem.*, **1990**, *94*, 4769.

[9] a) Meyer, F.; Khan, F.A.; Armentrout, P.B. *J. Am. Chem. Soc*., **1995**, *117*, 9740. b) Chen, Y.M.; Armentrout, P.B. *Chem. Phys. Lett*., **1993**, *210*, 123.

[10] Nakajima, A.; Kaya, K. *J. Phys. Chem. A* **2000**, *104*, 176.

[11] Weis, P.; Kemper, P.R.; Bowers, M. *J. Phys. Chem*. **1997**, *104*, 8207.

[12] Kroto, H.W.; Heath, J.R.; O'Brien, S.cc.; Curl, R.F.; Smalley, R.E. *Nature (London)*, **1985**, *318*, 162.

[13] Tast, F.; Malinowski, N.; Billas, I.M.L.; Heinebrot, M.; Martin, T.P., *Z. Phys. D: At., Mol. & Clusters*, **1997**, *40*, 351.

[14] a) Branz, W.; Billas, I.M.L.; Malinowski, N.; Tast, F.; Heinebrodt, M.; Martin, T.P. *J. Chem. Phys.*, **1998**, *109*, 3425. b) Martin, T.P.; Malinowski, N.; Zimmerman, U.; Naher, U.; Schaber, H.J., *J. Chem. Phys.* **1993**, *99*, 4210. c) Zimmerman, U.; Malinowski, N.; Naher, U.; Frank, S.; Martin, T.P., *Phys. Rev. Lett.* **1994**, *72*, 3542. d) Tast, F.; Malinowski, N.; Frank, S.; Heinebrot, M.; Billas, I.M.L.; Martin, T.P., *Phys. Rev. Lett.* **1996**, *77*, 3529.

[15] a) Clemmer, D.E.; Hunter, J.M.; Shelimov, K.B.; Jarrold, M.F. *Nature (London)*, **1994**, *372*, 248. b) Fye, J.L.; Jarrold, M.F., *Intl. J. Mass Spec.* ,**1999**, *187*, 507.

[16] a) Buchanan JW; Reddic JE, Grieves GA, Duncan, M.A, *J. Phys. Chem.* **1998**, *102*, 6390. b) Buchanan JW, Grieves GA, Flynn ND, Duncan, M.A. *Intl. J. Mass. Spectrom.*,**1999**, *187*, 617.

[17] Reddic, J.E.; Robinson, J.C.; Duncan, M.A. *Chem. Phys. Lett.*, **1997**, *279*, 203.

[18] Buchanan, J.W.; Grieves, G.A.; Reddic, J.E.; Duncan, M.A., *Intl. J. Mass. Spectrom.*, . **1999**, *182*, 323

[19] Pozniak, B.P.; Dunbar, R.C. *J. Am. Chem. Soc.* **1997**, *119*, 10439.

[20] a) Foster, N.R.; Buchanan, J.W.; Flynn, N.D.; Duncan, M.A. *Chem. Phys. Lett.*, **2001**, *341*, 476. b) Foster, N.R.; Grieves, G.A.; Buchanan, J.W.; Flynn, N.D.; Duncan, M.A. *J. Phys. Chem. A.*, **2000**, *104*, 11055.

[21] A. Klotz, P. Marty, P. Boissel, G. Serra, B. Chaudret, and J.P. Daudey. *Astron. Astrophys.* **1995**, *304*, 520.

[22] Allamandola, L.J.; Tielens, A.G.G.M.; Barker, J.R.; *Astrophys. J.*, **1985**, *290*, L25.

[23] Streitwieser Jr., A; Müller-Westerhoff, U. *J. Am. Chem. Soc.*, **1968**, *90*, 7364.

[24] Hayes, R.G.; Thomas, J.L. *J. Am. Chem. Soc.*, **1969**, *120*, 1891 b) Hodgson, K.O.; Mares, F.; Starks, D.F.; Streitwieser, A. Jr. *J. Am. Chem. Soc.*, **1973**, *95*, 8650. c) DeKock, C.W.; Ely, S.R.; Hopkins, T.E.; Bault, M.A. *Inorg. Chem.*, **1988**, *17*, 625.

[25] Kinsley, S.A.; Streitwieser, A., Jr.; Zalkin, A. *Organometallics*, **1985**, *4*, 52.

[26] Buchanan, J.W.; Reddic , J.E.; Grieves, G.A.; Duncan, M.A.; *J. Phys. Chem., A* **1998**, *102*, 6390.

[27] Yeh, C.S.; Pilgrim, J.S.; Robbins, D.L.; Willey, K.F.; Duncan, M.A., *Intl. Rev. Phys. Chem.* **1994**, *13*, 231.

[28] a) Dietz, T.G.; Duncan, M.A.; Powers, D.E.; Smalley, R.E:, *J. Chem. Phys*., **1981**, **74**, 6511. b) Duncan, M.A., *Ann. Rev. Phys. Chem.*, **1997**, *48*, 63.

[29] Wiley, W.C. and McLaren, I.H., *Rev. Sci. Instrum*., **1955**, *26*, 1150.

[30] a) Hoshino, K.; Kurikawa, T.; Takeda, H.; Nakajima, A.; Kaya, K., *J. Phys. Chem.* **1995**, *99*, 3053. b) Judai, K.; Hirano, M.; Kawamata, H.; Yabushita, S.; Nakajima, A.; Kaya, K., *Chemical Physics Lett*.**1997**, *270*, 23. c)Nagao, S.; Negishi, Y.; Kato, A.; Nakamura, Y.; Nakajima, A.; Kaya, K. *J. Phys. Chem. A* **1999**, *103*, 8909.

[31] Armentrout, P.B.; Hales, D.A.; Lian, L., *Adv. Metal & Semiconductor Clusters*, M.A. Duncan, ed., **1994**, Vol. 2, p.1 (JAI Press, Greenwich, CT).

[32] Simard, B.; Lebeault-Dorget, M.-A.; Marijnissen, A.; ter Meulen, J.J., *J. Chem. Phys.* **1998**, *108*, 9668.

[33] Foster, N.R.; Buchanan, J.W.; Flynn, N.D.; Duncan, M.A. *Chem. Phys. Lett.*, **2001**, *341*, 476

[34] Clemmer, D.E.; Hunter, J.M.; Shelimov, K.B.; Jarrold, M.F., *Nature* **1994**, *372*, 248.

[35] a) Branz, W.; Billas, I.M.L.; Malinowski, N.; Tast, F.; Heinebrodt, M.; Martin, T.P., *J. Chem. Phys*.**1998**, **109**, 3425.

[36] a) Nakajima, A.; Nagao, S.; Takeda, H.; Kurikawa, T.; Kaya, K., *J. Chem. Phys.* **1997**, 107, 6491. b) Kurikawa, T.; Nagao, S.; Miyajima, K.; Nakajima, A.; Kaya, K., *J. Phys. Chem. A* **1998**, *102*, 1743. c) Nagao, S.; Kurikawa, T.; Miyajima, K.; Nakajima, A.; Kaya, K., *J. Phys. Chem. A* **1998**, **102**, 4495. d) Nagao, S.; Negishi, Y.; Kato, A.; Nakamura, A.; Nakajima, A.; Kaya, K., *J. Phys. Chem. A* **1999**, *103*, 8909. e) Nakajima, A.; Kaya, K., *J. Phys. Chem. A* **2000**, *104*, 176.

[37] Buchanan, J.W.; Grieves, G.A.; Reddic, J.E.; Duncan, M.A., *Intl. J. Mass. Spectrom*., . **1999**, *182*, 323

[38] Schmitt, G.;. Kein, WS.; Fleischhauer, J.; Walbergs, U., *J. Organomet. Chem*. **1978**, *152*, 315.

[39] Morrison, W.H.; Ho, E.Y.; Hendrickson, D.N., *Inorg. Chem*. **1975**, *14*, 500.

[40] Klotz, A.; Marty, P.; Boissel, P.; de Caro, D.; Serra, G.; Mascetti, J.; de Parseval, P.; Deroualt, J.; Daudey, J.-P.; Chaudret, B., *Planet. Space Sci.* **1996**, *44*, 957.

b) Chaudret, B.; Le Beuze, A.; Rabaâ, H.; Saillard, J.Y.; Serra, G., *New J. Chem*. **1991**, *15*, 791.

[41] a) Wei, S.; Guo, B.C; Deng, H.T.; Kerns, K.; Purnell, J.; Buzza, S.A.; Castlemann, Jr. A.W., *J. Am. Chem. Soc*., **1994**, *116*, 4475. b). Pilgrim, J.S.; Brock L.R.; Duncan, M.A., *J. Phys. Chem.*, **1995**, *99*, 544. c) Yeh, C.S, Byun, Y.G.; Afzaal, S.; Kan, S.Z.; Lee, S.; Freiser, B.S.; Hay, P.J., *J. Am. Chem. Soc*., **1995**, *117*, 4042

[42] Wang, X.; Becker, H.; Hopkinson, A.C.; March, R.E.; Scott L.T.; Bohme, D.K., *Intl. J. Mass Spec.*, **1997**, *161*, 69.

[43] Fye, J.L.; Jarrold, M.F., *Intl. J. Mass Spec*. ,**1999**, *187*, 507.

[44] A. Cottrell, *Chemical Bonding in Transition Metal Carbides*, The Institute of Materials, London, **1995**.

[45] Bauschlicher, C.W.; Partridge, H.; S.R. Langhoff, *J. Phys. Chem*., **1992**, *96*, 3273.

[46] Kurikawa, T.; Negishi, Y.; Hayakawa, F.; Nagao, S.; Miyajima, K.; Nakajima, A.; Kaya, K. *J. Am. Chem. Soc*., **1998**, *120*, 11766.

[47] Greco, A.; Cesca, S.;Bertolini, G. *J. Org. Chem*., **1976**, *113*, 321. b) DeKock, C.W.; Ely, S.R.; Hopkins, T.E.; Brault, M.A. *Inorg. Chem* **1978**, *17*, 625. c) Ely, S.R.; Hopkins, T.E.; DeKock, C.W. *J. Am. Chem. Soc.* **1976**, *98*, 1624.

[48] Edelmann, F.T. *New J. Chem* **1995**, *19*, 535.

[49] S.G. Lias, "Ionization Energy Evaluation" in NIST Chemistry WebBook, NIST Standard Reference Database Number 69, Eds. W.G. Mallard and P.J. Linstrom, February 2000, National Institute of Standards and Technology, Gaithersburg MD, 20899 (http://webbook.nist.gov).